The Journal of Chemical Physics

RESEARCH ARTICLE | APRIL 06 2026

e^T 2.0: An efficient open-source molecular electronic structure program

Special Collection: Electronic Structure Software 2.0

Sarai Dery Folkestad ✉ ; Eirik F. Kjønstad ✉ ; Alexander C. Paul ; Rolf H. Myhre ; Riccardo Alessandro ; Sara Angelico ; Alice Balbi ; Alberto Barlini ; Andrea Bianchi ; Chiara Cappelli ; Matteo Castagnola ; Sonia Coriani ; Yassir El Moutaoukal ; Tommaso Giovannini ; Linda Goletto ; Tor S. Haugland ; Daniel Hollas ; Ida-Marie Høyvik ; Marcus T. Lexander ; Doroteja Lipovec ; Gioia Marrazzini ; Torsha Moitra ; Ylva Os ; Regina Paul ; Jacob Pedersen ; Matteo Rinaldi ; Rosario R. Riso ; Sander Roet ; Enrico Ronca ; Federico Rossi ; Bendik S. Sannes ; Anna Kristina Schnack-Petersen ; Andreas S. Skeidsvoll ; Leo Stoll ; Guillaume Thiam ; Jan Haakon M. Trabski ; Henrik Koch ✉

J. Chem. Phys. 164, 132501 (2026)
https://doi.org/10.1063/5.0309334

The Journal of Chemical Physics SOFTWARE pubs.aip.org/aip/jcp

e^T 2.0: An efficient open-source molecular electronic structure program

Cite as: J. Chem. Phys. 164, 132501 (2026); doi: 10.1063/5.0309334
Submitted: 27 October 2025 • Accepted: 2 March 2026 •
Published Online: 6 April 2026

Sarai Dery Folkestad,[1,a)] Eirik F. Kjønstad,[1,a)] Alexander C. Paul,[1] Rolf H. Myhre,[1,2] Riccardo Alessandro,[3] Sara Angelico,[1] Alice Balbi,[1] Alberto Barlini,[4] Andrea Bianchi,[4] Chiara Cappelli,[4] Matteo Castagnola,[1] Sonia Coriani,[5] Yassir El Moutaoukal,[1] Tommaso Giovannini,[6] Linda Goletto,[4] Tor S. Haugland,[1] Daniel Hollas,[7] Ida-Marie Høyvik,[1] Marcus T. Lexander,[1] Doroteja Lipovec,[1] Gioia Marrazzini,[4] Torsha Moitra,[5,8] Ylva Os,[9] Regina Paul,[1] Jacob Pedersen,[1,5] Matteo Rinaldi,[4] Rosario R. Riso,[1] Sander Roet,[1,10] Enrico Ronca,[3] Federico Rossi,[1] Bendik S. Sannes,[1] Anna Kristina Schnack-Petersen,[5] Andreas S. Skeidsvoll,[1,11] Leo Stoll,[1] Guillaume Thiam,[3] Jan Haakon M. Trabski,[1] and Henrik Koch[1,a)]

AFFILIATIONS

[1]Department of Chemistry, Norwegian University of Science and Technology, 7491 Trondheim, Norway
[2]Development Centre for Weather Forecasting, Norwegian Meteorological Institute, Oslo, Norway
[3]Dipartimento di Chimica, Biologia e Biotecnologie, Università Degli Studi di Perugia, 06123 Perugia, Italy
[4]Scuola Normale Superiore, Piazza dei Cavalieri, 7, 56126 Pisa PI, Italy
[5]DTU Chemistry—Department of Chemistry, Technical University of Denmark, DK-2800 Kongens Lyngby, Denmark
[6]Department of Physics, University of Rome Tor Vergata and INFN, Via della Ricerca Scientifica 1, 00133 Rome, Italy
[7]Centre for Computational Chemistry, School of Chemistry, University of Bristol, Cantocks Close, Bristol BS8 1TS, United Kingdom
[8]Department of Physical and Theoretical Chemistry, Faculty of Natural Sciences, Comenius University, SK-84215 Bratislava, Slovakia
[9]Department of Chemistry, The Arctic University of Norway, 9037 Tromsø, Norway
[10]Structural Biochemistry, Bijvoet Centre for Biomolecular Research, Utrecht University, 3584 CG Utrecht, The Netherlands
[11]Department of Physics and Technology, University of Bergen, Bergen, Norway

Note: This paper is part of the Special Topic on Electronic Structure Software 2.0.
[a)]**Authors to whom correspondence should be addressed:** sarai.d.folkestad@ntnu.no; eirik.f.kjonstad@gmail.com; and henrik.koch@ntnu.no

ABSTRACT

The e^T program is an open-source electronic structure program with an emphasis on performance and modularity. As its name suggests, the program features extensive coupled cluster capabilities, performing well compared to other electronic structure programs and, in some cases, outperforming commercial alternatives. However, e^T is more than a coupled cluster program; other models based on wave function theory (such as full and reduced-space configuration interaction and a variety of self-consistent field models) and density functional theory are supported. The second major release of the program, e^T 2.0, has specialized functionality for strong light–matter coupling conditions. In addition, it includes a wide range of optimizations and algorithmic improvements, as well as new capabilities for exploring potential energy surfaces and for modeling experiments in the ultraviolet and X-ray regimes. Molecular gradients are now available at the coupled cluster level, and high-accuracy spectroscopic simulations are available at reduced computational cost within the multilevel coupled cluster and multiscale frameworks. We present the modifications to the program since its first major release, e^T 1.0, highlighting some notable

new features and demonstrating the performance of the new version relative to the first release and to other established electronic structure programs.

 https://doi.org/10.1063/5.0309334

I. INTRODUCTION

Research in electronic structure theory relies on efficient, reliable, and maintainable software. Over the past six decades, a large number of programs have emerged to address this need, some focusing on specific electronic structure methods and others adopting a broad and ambitious scope; see for instance Refs. 1–21. A massive amount of work has been invested in the development of these programs. In many cases, what may seem like simple calculations (e.g., evaluating some molecular property such as the dipole moment) often depend on thousands of lines of code. This can make extending the software a daunting and time-consuming task, emphasizing the need for adherence to best practices in software development.

To remain useful, software must also continually adapt to new computing paradigms to follow the evolution of computer hardware and architecture. Perhaps the most important shift in recent years has been from serial to parallel programming, where high performance gains are achieved by exploiting the large number of central processing unit (CPU) cores in modern computers, and more recently toward accelerator-based, heterogeneous architectures. This shift is reshaping high-performance computing (HPC) facilities around the world, driven to a large extent by developments in artificial intelligence and machine learning. Adapting (or rewriting) software to accommodate new hardware paradigms, such as a transition from single-node CPU algorithms toward multi-node CPU (with shared or distributed memory) or graphical processing unit (GPU) algorithms, is central to the productivity of the field of quantum chemistry.[22]

The size of electronic structure programs, combined with developments in hardware, highlights the need for code bases that are easily adaptable. This fact has led some to argue that electronic structure software requires commercialization to meet the need for software expertise and maintenance.[23] Others have emphasized the importance of open-source software[24] and the broad adoption of software best practices to minimize the technical debt (and thus the time taken away from research) that results from poorly written and poorly maintained code bases.[22]

The present work is in line with the latter perspective. The e^T program is an open-source electronic structure program under the GNU General Public License v3.0 (GPLv3) with a developer community that places emphasis on code quality, rigorous testing, and maintainability, reflecting our belief that, under these conditions, large code bases can be developed and successfully managed by the scientific community. While initially focusing on coupled cluster methods, e^T is today a full-fledged electronic structure program with a wide variety of features.

The e^T program is an object-oriented code, primarily written in Fortran 2018. The code is especially optimized for modern CPU nodes with fast (shared) memory and input/output (I/O), parallelized through OpenMP and extensive use of the BLAS and LAPACK libraries. e^T 2.0 can be used on Unix-based operating systems (macOS and Linux). We support modern versions of the GNU compilers (10.4 or newer) and Intel compilers (ifx, icx, and icpx 2024.0 or newer). Installation instructions for the program and dependencies are provided in the README.md file, and reproducible installation recipes for both GNU and Intel compilers are available as public Dockerfiles.[25] The code is hosted on GitLab (www.gitlab.com/eT-program/eT) and publicly developed, with both code review and a development version of the code available to the public, in addition to the latest stable release. The user manual, along with news about the community, is available on the website (www.etprogram.org). The e^T community is, therefore, fully open to collaboration and committed to transparency.

In this paper, we present the second major release of the program, e^T 2.0, highlight the improved performance of the program compared to its first release, and showcase several significant features.

II. PROGRAM STRUCTURE AND FEATURES

The e^T 2.0 program offers a wide range of features for electronic structure calculations. Its structure reflects the subtasks involved in such calculations, with dedicated modules (more precisely, classes in object-oriented terminology) with distinct and well-defined responsibilities. High-level examples include the classes referred to as *engines* (which drive calculations by invoking a sequence of *tasks*), *solvers* (which solve model equations), and *wave functions* (which implement the particular model equations). This modular structure makes it easy to extend the program and reuse existing code when designing new features. It also facilitates interfacing with other codes that may invoke high-level modules to obtain the desired electronic structure information (see, e.g., Ref. 26).

Compared with its first release,[27] the new version of e^T includes various algorithmic improvements, in addition to extensions in terms of which areas of chemistry can be explored. In particular, it has been shown that molecular properties can be manipulated by placing molecules between closely spaced mirrors, resulting in a strong coupling of electrons and photons. These situations are described through cavity quantum electrodynamics (QED) methods, which incorporate the coupling of the electronic structure to one or several photonic modes. The e^T program now provides energies at both mean-field and correlated levels of theory for investigating such strong-coupling chemistry.[28–34] The QED functionality has also been extended to use plasmonic modes[35,36] that are calculated separately for the nanostructure and imported into the e^T program. This enables the study of strong coupling between localized surface plasmons and molecules.

The new version also enables a broader set of applications in the areas of spectroscopy and photochemistry. For example, ground- and excited-state equilibrium geometries, as well as vibrational frequencies, calculated using analytical nuclear gradients, can now

be efficiently determined at the Hartree–Fock (HF) and coupled cluster singles and doubles (CCSD) (ground and excited states)[37] levels of theory. Furthermore, molecular gradients at the QED-HF level[38,39] are also available. Hence, the program can be used to explore new regions of the potential energy landscapes, as well as for ground- and excited-state Born–Oppenheimer molecular dynamics calculations.[37,40]

The new version enables fast simulation of absorption spectra with coupled cluster theory. These features have also been extended in new directions, such as the determination of triplet states and improved support for multilevel coupled cluster calculations. In e^T 2.0, excitation energies and transition moments can also be computed with time-dependent Hartree–Fock (TDHF) theory. The time-dependent coupled cluster (TDCC)[41] method has been extended with the time-dependent equation-of-motion coupled cluster (TD-EOM-CC) technique,[41,42] further extending the program's capabilities of simulating electron dynamics with explicit pulses.

e^T 2.0 also has extended support for other established electronic structure models. The full configuration interaction (FCI) model, both in a full or in an active orbital space, has been added to the program. Within coupled cluster theory, the coupled cluster singles, doubles, and triples (CCSDT) model is now available for both ground- and excited-state calculations. At the Hartree–Fock level, we have expanded e^T to include the restricted open-shell model, implemented through the constrained unrestricted Hartree–Fock approach.[43] Kohn–Sham density functional theory (DFT) has been added for ground-state calculations using the local density approximation (LDA), generalized gradient approximation (GGA), and hybrid functionals.[44,45] The DFT grid is constructed using the widely employed Lebedev grid,[46] with the radial quadrature proposed in Ref. 47.

The e^T program now has broadened support for molecular properties. Dipole and quadrupole moments are available with the Hartree–Fock models, the coupled cluster models (except CCSDT), and with FCI and complete active space configuration interaction (CASCI). Static and frequency-dependent (dipole) polarizabilities can be calculated at the Hartree–Fock and coupled cluster levels of theory, and nuclear magnetic resonance (NMR) shielding parameters are available with Hartree–Fock. Dipole oscillator strengths in various gauges (length, velocity, and mixed), as well as rotatory strengths of electronic circular dichroism, in both length and modified velocity gauges, are available with the CCSD model and with restricted closed-shell Hartree–Fock and QED-Hartree–Fock.

Some of the program features rely on external open-source software packages and libraries. Integrals are provided through one of three integral libraries: Libcint[48] is the default integral library, but e^T can also be used with integrals from Libint[49] or PhasedInt[50] through a unified interface that allows for a seamless exchange of integral providers. Optionally, polarizable continuum environments can be included through the PCMSolver library,[51] and the LibXC library[52,53] enables DFT calculations. However, to use most of the features in e^T, only one integral library must be installed (i.e., Libcint, Libint, or PhasedInt).

On the algorithmic front, the e^T program offers a range of solvers that ensure efficient and robust convergence for the variety of equations that must be solved. Since the release of the first major version, the program has significantly improved in this regard. The program now has support for a trust-region algorithm[54–56] that is currently used for quadratically convergent self-consistent field (SCF) optimizations, occupied and virtual orbital localization,[57] and for SC-QED-HF optimization.[31] However, the trust-region solver can be used for any optimization problem, as long as the functional, its gradient, and the linear transformation by the (approximate) Hessian are implemented. Similarly, the e^T program also provides Davidson-like reduced space solvers[58,59] that can be used for any eigenvalue or linear equation problem, as long as the linear transformation is provided. These solvers are flexible and only require setting up a transformation object and passing it along to the solver, facilitating future extensions.

Particular improvements have been made for the calculation of excited states with the perturbative coupled cluster models (CC2[60] and CC3[61,62]). For these models, the eigenvalue problem may be recast into a nonlinear eigenvalue problem in a reduced parameter space. In e^T 1.0, these equations were solved using a DIIS algorithm[63,64] that suffers from the occasional appearance of duplicate roots and does not ensure convergence to the lowest-energy solutions. In e^T 2.0, a nonlinear Davidson solver that avoids both these problems is available. Furthermore, for CC3, the multimodel solvers by Kjønstad *et al.*[65] can be used for both the ground- and excited-state equations. These solvers improve convergence, resulting in significant computational savings in CC3 calculations. Finally, the code also features a band-Lanczos solver[42] and a damped linear response solver for resonance-convergent response properties and spectra.[66] In general, the solvers in e^T are built using general tools that make it easy to implement new solvers.

The robustness of the program is supported by a broad and comprehensive suite of tests, and we have made several improvements in this direction since the original release. Our tests are optimized for speed, single out selected features for testing, and target near-complete code coverage (monitored using Coveralls[67]). Our code repository is connected to a CI/CD setup that automatically checks the validity of the code upon every commit to the repository, both in the development and the release branches. The test set includes a large number of integration tests (using the Runtest library[68]) and some unit tests,[69] checking a range of possible configurations of the program (with different compilers, dependencies, compiler flags, etc.). The test suite provides confidence in the correctness of the program and aids in refactoring and extending the program with the knowledge that new bugs are likely not being introduced in existing features.

III. HIGHLIGHTED PROGRAM CAPABILITIES

A. Quantum-electrodynamical electronic structure theory

Strong coupling between electromagnetic fields and molecular systems gives rise to hybrid light–matter states known as polaritons.[70–73] Due to photon–molecule entanglement, polaritons exhibit unique properties that cannot be explained by their uncoupled counterparts.[74–76] Crucially, they can be engineered by tuning the photonic component, enabling noninvasive modulation of matter properties.[77–79] Optical cavities, composed of mirrors that confine the electromagnetic field within a small quantization volume, provide an optimal platform for achieving strong light–matter

coupling.[80–82] The interaction strength increases as the quantization volume decreases, driving experimental efforts toward extreme field confinement. Plasmonic nanocavities currently achieve the strongest coupling, with quantization volumes below a single nm^3.[83,84]

By engineering cavity mirrors, key field properties—such as frequency, shape, and polarization—can be controlled.[85] Polaritonic effects have been experimentally observed in absorption spectra, photochemical reaction rates, and conductivity.[82,86–89] Notably, it has been shown that photonic coupling to molecular vibrations can catalyze, slow down, or induce selectivity in chemical reactions.[86–88] However, reproducing experimental results remains challenging,[90] highlighting the need for theoretical modeling to understand the complex light–matter interplay. Developing *ab initio* electron–photon methods is an important step toward understanding cavity effects. Since photons play a fundamental role, they must be treated as quantum particles following QED principles. The first *ab initio* methodology that adopted standard quantum chemistry methods for electron–photon systems was quantum electrodynamical density functional theory (QEDFT).[91–93] While computationally efficient, QEDFT inherits functional limitations in describing electron–electron and electron–photon correlations. Subsequently, we have developed and implemented QED-Hartree–Fock (QED-HF),[28,29] strong coupling QED-HF (SC-QED-HF),[30–32] QED-coupled cluster (QED-CC),[28,29] QED-FCI, and complete active space configuration interaction (QED-FCI/QED-CASCI), as well as the cavity Born–Oppenheimer (CBO) approximation for all electronic structure methods,[33] in the e^T program. These methods now enable the computation of both ground- and excited-state properties of molecules within optical cavities. In Fig. 1, for example, we display how the excitation energies of a furan molecule depend on the cavity frequency ω. The excited-state results are computed

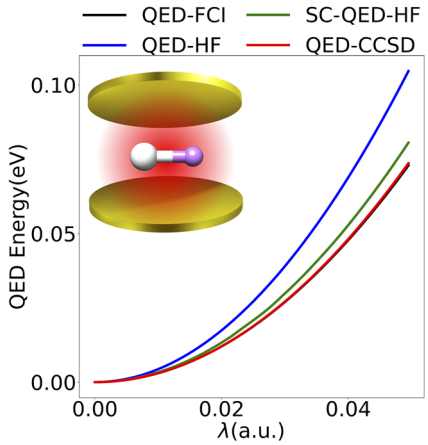

FIG. 2. Dispersion of the ground-state energy of LiH using the aug-cc-pVDZ basis with respect to the light–matter coupling, λ. While QED-CCSD clearly outperforms QED-HF and SC-QED-HF, all the implemented methods capture the qualitative behavior of the function.

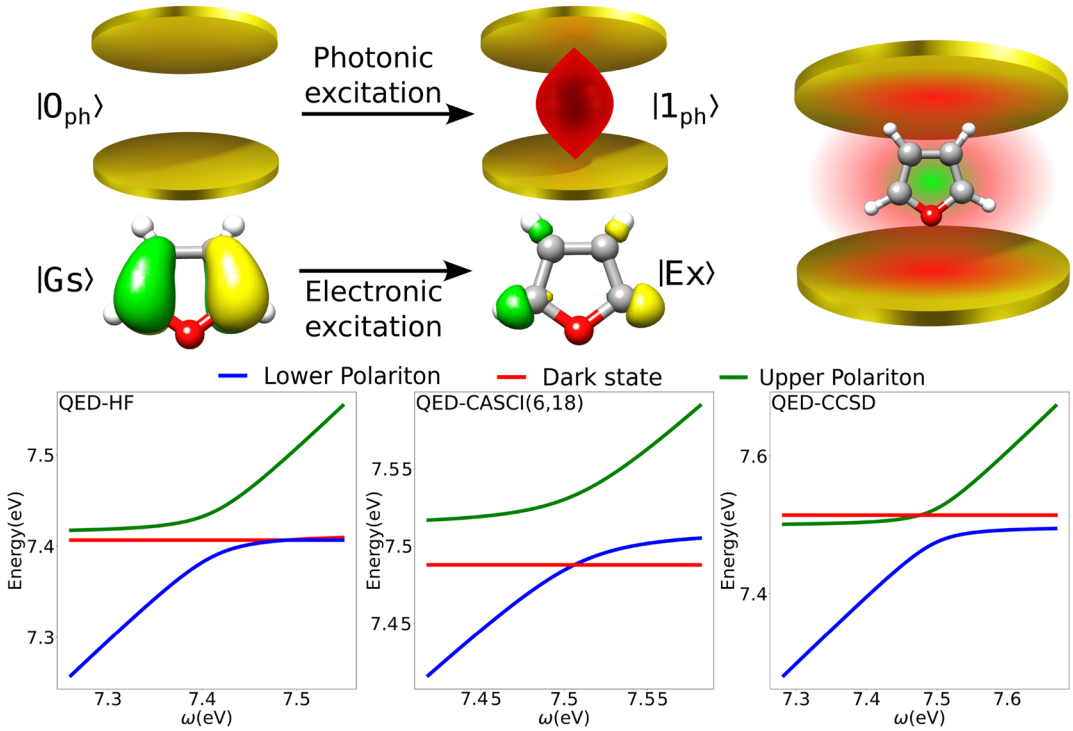

FIG. 1. Dispersion of the excitation energies of furan using the aug-cc-pVDZ basis in an optical cavity, as a function of the cavity frequency, ω. On the top panel of the image, we display the orbital transition mainly featured in the excitation. On the bottom panel of the figure, we show the formation of the lower and upper polaritons.

using QED-HF, QED-CAS, and QED-CCSD. For all three cases, we observe that when the photonic energy is resonant with a molecular excitation, an avoided crossing is observed. The accuracy of the excitation energies increases when going from HF to CCSD, but the qualitative picture is the same, independent of the chosen approach.

In Figs. 2 and 3, we show the cavity frequency (ω) and light–matter coupling (λ) dispersions for the ground-state energy of lithium hydride as computed using mean-field methods (QED-HF, SC-QED-HF) and correlated methods (QED-CCSD, QED-FCI). While all approaches capture the qualitative behavior of the λ energy dispersion, the same is not true for the ω dispersion. In particular, we notice that the QED-HF ground-state energy is independent of the field frequency. This problem is solved using the SC-QED-HF mean-field approach, which also provides a fully consistent set of molecular orbitals.[30,31]

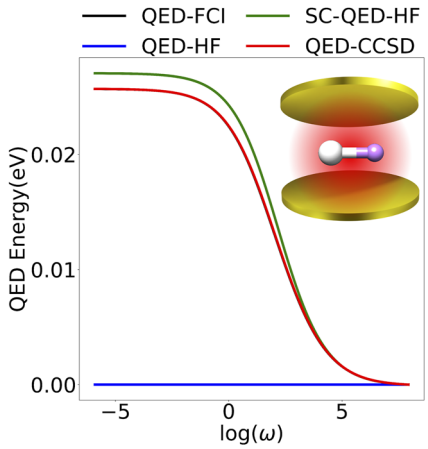

FIG. 3. Dispersion of the ground-state energy of LiH using the aug-cc-pVDZ basis with respect to the cavity frequency, ω. The QED-HF energy is completely independent of ω, while SC-QED-HF, despite being a mean-field approach, reproduces the QED-FCI behavior qualitatively. Excellent agreement is observed between QED-CCSD and QED-FCI results.

B. Real-time time-dependent equation-of-motion coupled cluster theory

Real-time time-dependent equation-of-motion coupled cluster theory parametrizes time dependence with the linear coefficients of the EOM-CC states. This allows one to compute the electronic time evolution of a system, its observables, and the populations of excited states. The TD-EOM-CC approach has applications in, for example, the simulations of ultrafast phenomena such as stimulated X-ray Raman scattering.[42,94] The TD-EOM-CC method can provide greater numerical stability[95] compared to the TDCC method, which was already present in e^T 1.0. In addition to the already present numerical integrators, adaptive time-stepping capabilities and Dormand–Prince integrators [with orders 5(4) and 8(5,3)][96,97] have been added to the new version of the program.[42]

As an illustration of these capabilities, we consider the *p*-nitroaniline molecule in the presence of an external electric field. Figure 4 shows the density difference relative to the ground-state electron density at different time steps. The molecular geometry is provided in the supplemental material of Ref. 28, and it was optimized at the DFT/B3LYP level of theory using a 6-31+G* basis set.[99] The time-dependent state is propagated for 800 a.u., and the chosen electric field has a Gaussian envelope with a width of 5 a.u. The chosen carrier angular frequency is 0.166 152 a.u., which corresponds to the excitation energy between the ground state and the second excited state. The peak strength was set to 1 a.u., the envelope has a central time set to 80 a.u., and the polarization was oriented in the $[1, 1, 1]$ (non-normalized) direction.

C. Ground- and excited-state molecular geometry optimization, harmonic frequencies, and normal modes

Identifying stationary structures is useful in various contexts, allowing the user to inspect vibrational modes and frequencies and potentially aiding in the interpretation of excited-state dynamics, as well as in isolating spectral signatures by extraction of spectra at stationary points, for example, for interpreting time-resolved X-ray spectra. In e^T 2.0, we have implemented ground- and excited-state singlet gradients at the EOM-CCSD level of

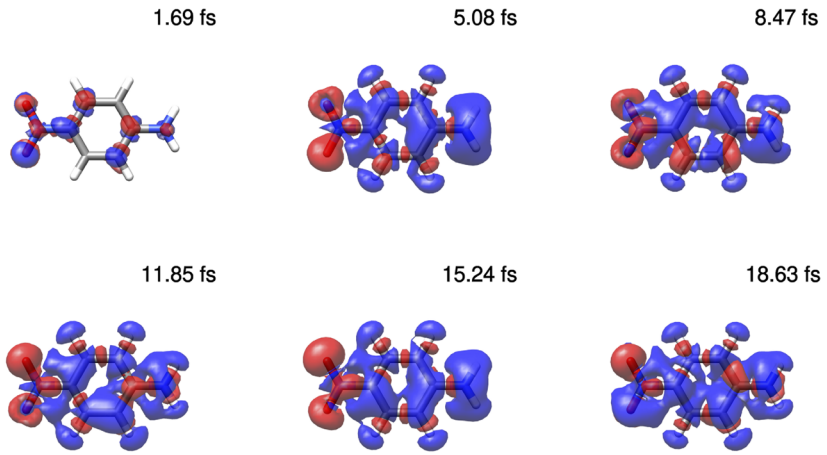

FIG. 4. Time evolution of the isodensity surfaces after subtracting the ground-state electron density, plotted using UCSF Chimera.[98] The calculation was performed with TD-EOM-CCSD/aug-cc-pVDZ. The system is a molecule of *p*-nitroaniline in the presence of an external electric field. The red surface depicts the isosurface at a 0.001 contour level, while the blue one refers to the −0.001 contour level. The interaction with the external electric field induces a migration of electrons that leads to an increase of negative charge on the nitro group, while the amino group becomes more positively charged with respect to the ground state.

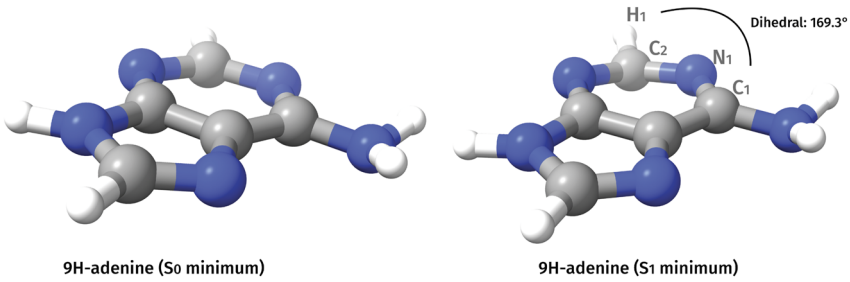

FIG. 5. An S_0 and an S_1 minimum in 9H-adenine determined with EOM-CCSD/cc-pVDZ. In the S_1 minimum, we observe a puckering of the C2 carbon atom that is not present in the S_0 minimum.

theory (both for valence and core excited states),[37] allowing for easy determination of stationary structures as well as harmonic frequencies, associated normal modes, and Wigner samples at 0 K. The new version of the program now also features a more robust Broyden–Fletcher–Goldfarb–Shanno (BFGS) optimizer that uses redundant internal coordinates[100] and rotational coordinates.[101] In this way, optimization of single-molecule systems, the orientation of fragments, and cavity-induced orientation effects (in QED-HF) are made possible. In Fig. 5, we provide an illustration of these new capabilities for the ground- and excited-state minima in 9H-adenine determined with the EOM-CCSD model. Associated harmonic frequencies are given in Tables I and II.

D. Modeling UV–vis and X-ray absorption and photoelectron spectroscopy

Modeling spectroscopies with coupled cluster theory has been a primary driver for developments in e^T. One-photon absorption and photoelectron spectra can be generated in the ultraviolet (UV)-visible and X-ray regions of the spectrum. Core excitations are obtained using the core–valence separation (CVS)[102,103] approximation, and ionization potentials are generated through the inclusion of a noninteracting orbital into the excited-state calculation, with intensities obtained through the use of Dyson orbitals.[104–108]

In Figs. 6 and 7, we have plotted the core (X-ray) and valence (UV) absorption and photoelectron spectra of the penta-2,4-dieniminium cation (PSB3, see Fig. 8). The calculations are performed with the CCSD and CC3 models. The geometry of PSB3 is optimized at the CCSD level of theory, and the CCSD spectra are also generated using 40 (NEXAFS) and 100 (UV) geometries obtained from a 0 K Wigner sample (see, e.g., Ref. 109) of geometries around the S_0 minimum.

TABLE I. Harmonic frequencies (ω) for the ground-state equilibrium geometry of 9H-adenine determined with EOM-CCSD/cc-pVDZ.

Mode	ω (cm^{-1})	Mode	ω (cm^{-1})	Mode	ω (cm^{-1})
1	3736	14	1380	27	697
2	3702	15	1337	28	673
3	3606	16	1277	29	624
4	3285	17	1273	30	581
5	3217	18	1165	31	541
6	1709	19	1097	32	527
7	1694	20	1059	33	499
8	1640	21	1000	34	476
9	1572	22	950	35	465
10	1548	23	910	36	302
11	1488	24	882	37	275
12	1444	25	818	38	220
13	1394	26	731	39	170

TABLE II. Harmonic frequencies (ω) for the excited-state minimum of 9H-adenine determined with EOM-CCSD/cc-pVDZ.

Mode	ω (cm^{-1})	Mode	ω (cm^{-1})	Mode	ω (cm^{-1})
1	3704	14	1312	27	638
2	3696	15	1273	28	590
3	3576	16	1254	29	572
4	3302	17	1165	30	529
5	3273	18	1097	31	470
6	1654	19	1059	32	458
7	1643	20	1000	33	414
8	1602	21	926	34	375
9	1564	22	796	35	298
10	1509	23	735	36	256
11	1440	24	714	37	238
12	1376	25	693	38	161
13	1334	26	660	39	147

E. Multilevel coupled cluster theory

For the calculation of intensive properties in molecular systems that are too large to be considered with standard coupled cluster methods, multilevel or multiscale (embedding) methods can be used.[112–116] In these approaches, an active region, or a set of active orbitals, is modeled with higher accuracy than the rest of the molecular system. In multiscale models, the environment is treated classically—for instance, with molecular mechanics (MM)[112] or as a polarizable continuum.[113,117] In multilevel models, different approximate levels of quantum mechanics (QM) are used for different orbital spaces.

The e^T program provides a range of multilevel and multiscale features. In particular, e^T provides an efficient implementation of the polarizable QM/MM method based on the fluctuating-charge force field,[118–120] and the multilevel coupled cluster and Hartree–Fock models, all of which are particularly powerful for spectroscopic and response properties.[121–123]

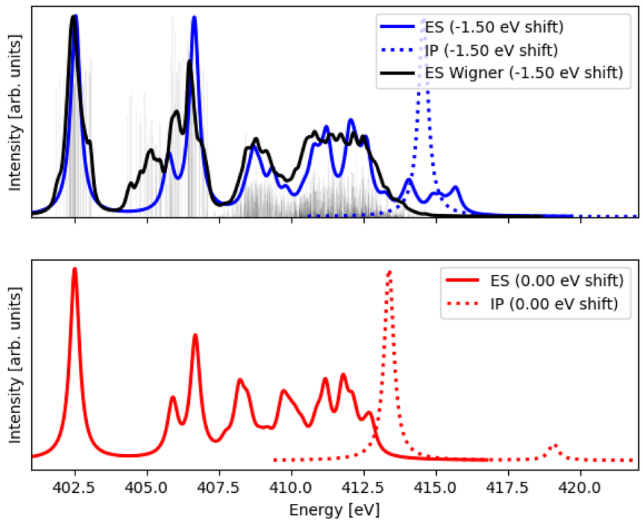

FIG. 6. Nitrogen K-edge excitation energies (ES) and ionization potentials (IP) for PSB3, calculated at the CCSD/aug-cc-pVDZ (top) and CC3/aug-cc-pVDZ (bottom) levels of theory. The NEXAFS and XPS peaks are rescaled separately. For the CCSD/aug-cc-pVDZ spectrum, the NEXAFS obtained from a Wigner sampling ($n = 40$) is shown. The CCSD spectra are shifted by −1.5 eV. A Lorentzian broadening is applied, with 0.4 eV FWHM for the S0-geometry calculations and 0.2 eV FWHM for the Wigner-sampling calculations.

In multilevel coupled cluster theory, the cluster operator is partially (MLCC) or fully (CC-in-HF) restricted to an active orbital space. For instance, in e^T 2.0, excitation energies can be calculated with MLCC2 and MLCCSD. In Table III, we present excitation energies of the betaine-30 molecule (see Fig. 9), calculated with CC2, CCSD, MLCC2, and MLCCSD. The wall time to calculate a single excitation energy with CCSD/aug-cc-pVDZ is around 137 h, and the full 2 TB of memory allocated for the calculation is utilized. An MLCCSD calculation, using approximate correlated natural transition orbitals (CNTOs)[110,111] to select the active orbital space, yields an excitation energy with an error of less than 10 meV in less than 4 h, and the memory usage is more than halved.

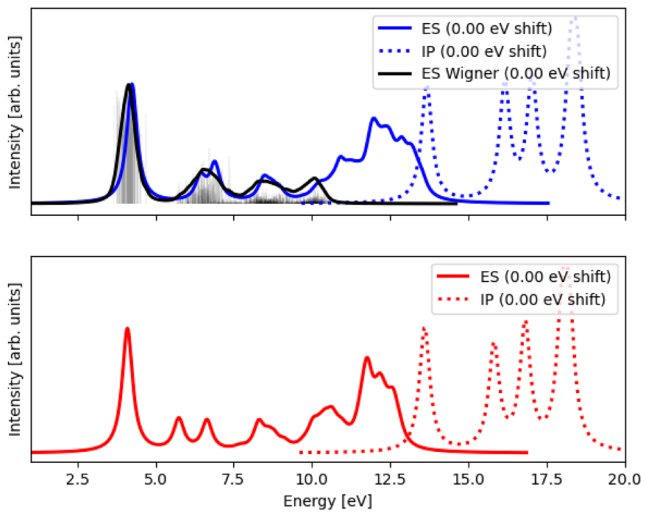

FIG. 7. Excitation energies (ES) and ionization potentials (IP) for PSB3, calculated at the CCSD/aug-cc-pVDZ (top) and CC3/aug-cc-pVDZ (bottom) levels of theory. The absorption and photoelectron spectra are rescaled separately. For the CCSD/aug-cc-pVDZ spectrum, the UV spectrum obtained from a Wigner sample ($n = 100$) is shown (with states limited to <10 eV). A Lorentzian broadening is applied, with 0.4 eV FWHM for the S0-geometry calculations and 0.2 eV FWHM for the Wigner sample calculations.

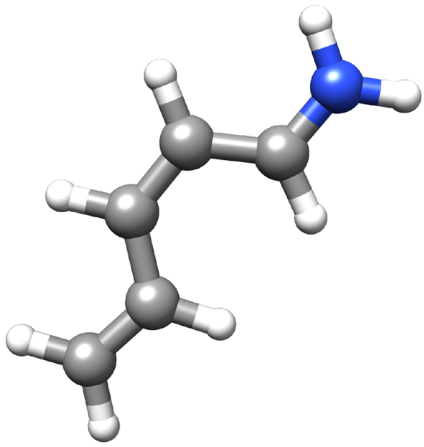

FIG. 8. The penta-2,4-dieniminium cation (PSB3) plotted using UCSF Chimera.[98]

In Fig. 10, the X-ray absorption spectrum of a water molecule in liquid water is modeled by use of CCSD-in-HF and CC3-in-HF. The core-excited water molecule and its four closest neighbors are included in the coupled cluster calculation, while the remaining molecules in the water cluster are modeled with a frozen Hartree–Fock density. The aug-cc-pVDZ basis is used for the five water molecules included in the coupled cluster calculation; the cc-pVDZ basis is used for the rest. The single snapshot in Fig. 10 echoes the findings of Ref. 121, where it was shown that the inclusion of triple excitations in the cluster operator is necessary to model the relative intensities between the main- and post-edges of the spectrum.

TABLE III. The lowest excitation energy, ω, of betaine-30 calculated with CC2, CCSD, MLCC2, and MLCCSD using the aug-cc-pVDZ basis. The active orbital space used in the MLCC2 and MLCCSD calculations consists of 40 occupied and 400 virtual orbitals and was determined using approximate correlated natural transition orbitals (CNTOs).[110,111] In total, there are 102 occupied and 1102 virtual orbitals (under the frozen core approximation). The calculations were done on two Intel Xeon Platinum 8380 CPUs (2.30 GHz), using 20 threads and 2 TB memory. The Cholesky decomposition threshold is 10^{-3}. The reported wall times are for the full calculation, including the determination of the reference state.

Model	ω (eV)	Wall time (h)	Peak memory usage
Low memory CC2	1.2157	7.1	2.0 TB
MLCC2	1.2918	2.0	365.3 GB
CCSD	1.7000	137.5	2.0 TB
MLCCSD	1.7064	3.7	868.1 GB

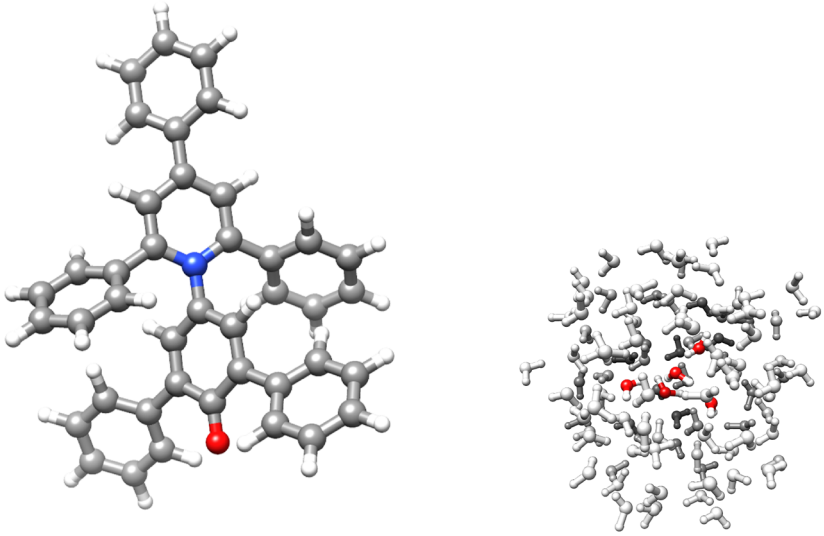

FIG. 9. The betaine-30 molecule and a water cluster plotted using UCSF Chimera.[98]

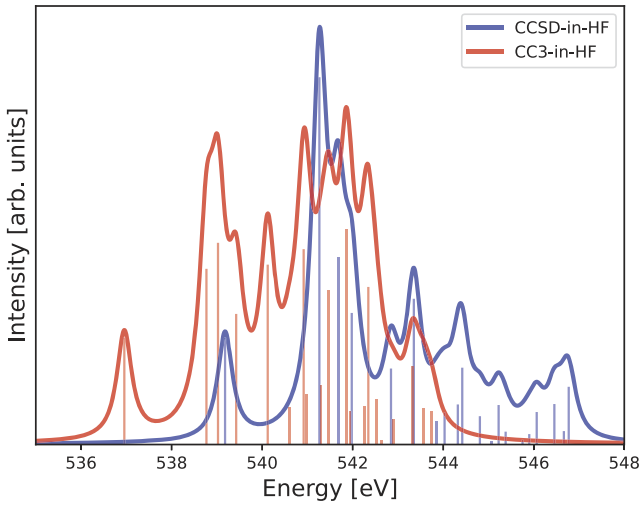

FIG. 10. X-ray absorption spectrum of a water molecule at the center of a water cluster, calculated at the CCSD-in-HF and CC3-in-HF levels of theory. The aug-cc-pVDZ basis is used for the five central water molecules, while the cc-pVDZ basis is used for the rest of the water cluster. The CCSD and CC3 spectra are normalized separately, such that the first peak has the same intensity for both models. A Lorentzian broadening with 0.4 eV FWHM is used.

The coupled cluster implementation in e^T is based on Cholesky-decomposed electron repulsion integrals. In multilevel calculations of this type, where a large part of the molecular system is described by a frozen Hartree–Fock density, the number of Cholesky vectors can be significantly reduced if one targets accuracy in the reduced active molecular orbital basis during the decomposition. This is done through the method-specific screening procedure described in Refs. 124 and 125, where the accuracy of the integrals in the active (reduced) molecular orbital (MO) basis is targeted, rather than in the full orbital space. For the water cluster calculations, the standard decomposition yields $n_J = 12\,689$ Cholesky vectors, while with active-space screening, $n_J = 1195$ Cholesky vectors are obtained, reducing the cost of the subsequent coupled cluster calculation. In Table IV, we report wall-time comparisons of the two decompositions and of the final CCSD-in-HF calculations. In Fig. 11, we show that the two X-ray absorption spectra generated with CCSD-in-HF, using different Cholesky decompositions, are nearly identical.

F. Efficient solvers for high-level coupled cluster theory

In e^T 2.0, several new solvers have been added that facilitate new calculations or significantly speed up convergence. In the calculation of excited states with the perturbative coupled cluster models (CC2 and CC3), the eigenvalue problem may be recast into a non-linear eigenvalue problem in a reduced parameter space. In e^T 1.0, these equations were solved using a DIIS algorithm, which suffers from the occasional appearance of duplicate roots and does not ensure convergence to the lowest-energy solutions. In e^T 2.0, a non-linear Davidson solver that avoids both these problems is available. Furthermore, for the CC3 model, an efficient multimodel solver based on the Olsen algorithm can be used.[65,126] The multimodel Olsen solver exploits the lower-level CCSD model to accelerate

TABLE IV. Cholesky decomposition wall time and the number of Cholesky vectors (n_J) for an X-ray absorption spectra (XAS) calculation of a water molecule in liquid water. Calculations are reported using the standard decomposition procedure and a decomposition targeting accuracy in the electron repulsion integrals in the reduced-space MO basis. The decomposition time (t_{CD}), the number of Cholesky vectors (n_J), and the total computational time for the XAS calculation (t_{total}) are given.

Type	n_J	t_{CD} (s)	t_{total} (h)
Standard	12 689	179	6.4
MO-screened	1195	17	4.1

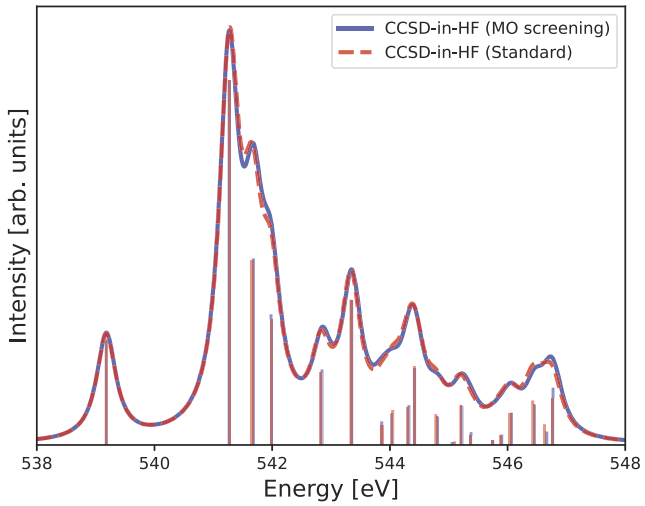

FIG. 11. Comparison of the X-ray absorption spectra of a water molecule in liquid water calculated with CCSD-in-HF/aug-cc-pVDZ using the standard and MO-screened Cholesky decompositions. A Lorentzian broadening with 0.4 eV FWHM is used.

convergence of the CC3 excited-state equations with the Olsen algorithm.[126] Similarly, for CC3 ground-state and response equations, a quasi-Newton solver that uses the CCSD Jacobian, rather than the orbital differences, to approximate the CC3 Jacobian, improves convergence.

In Table V, we compare timings of the CC3/aug-cc-pVDZ calculation of nicotine ($C_{10}N_2H_{14}$, 402 MOs) using e^T 1.0 and e^T 2.0. The overall wall time to determine the ground-state amplitudes [$\boldsymbol{t}$ and $\bar{\boldsymbol{t}}$ determined from Eqs. (A3) and (A12)] is more than halved in e^T 2.0. The ground-state and left amplitude equations have been optimized following the release of e^T 1.0; that is, in constructing $\boldsymbol{\Omega}$ and performing the linear transformation by $\boldsymbol{A}^T$, see the Appendix. However, the computational savings are primarily a result of changing the default solver to the multimodel Olsen solvers,[65] which approximately halve the number of $\boldsymbol{\Omega}$ constructions and linear transformations by $\boldsymbol{A}^T$, compared to the pure DIIS-accelerated algorithms used in e^T 1.0.

For excited states, CC3 calculations can be performed with three different solvers: a DIIS-accelerated steepest-descent algorithm, a nonlinear Davidson algorithm, or a multimodel Olsen algorithm. In Table VI, we report timings comparing the different algorithms when we calculate a single excited state with e^T 2.0. The DIIS and Olsen algorithms require fewer transformations than the nonlinear Davidson algorithm and, therefore, significantly reduce the wall time. This is especially pronounced for the right excited state, for which the initial guesses are less accurate; the left excited states are calculated with the right excited states as the initial guesses. In addition to optimizations of the $\boldsymbol{\Omega}$ construction and the linear transformation by $\boldsymbol{A}^T$, we have optimized the transformation by $\boldsymbol{A}$ since the release of e^T 1.0. For nicotine, CC3/aug-cc-pVDZ, the average wall time of an $\boldsymbol{A}$ transformation is 1 h 30 min with e^T 1.0 and 1 h 20 min with e^T 2.0.

From these calculations, the DIIS solver seems competitive, especially compared to the nonlinear Davidson solver. This picture, however, changes when one calculates several excitation energies. In Table VII, we report the calculation of ten excitation energies of the PSB3 molecule. The DIIS solver is the least efficient, and it also skips a root that is identified with both the nonlinear Davidson and the multimodel Olsen algorithms (compare roots 9 and 10 in Table VI). Both for nicotine and PSB3, the multimodel Olsen algorithm proves to be the more efficient algorithm for the CC3 model.

TABLE V. CC3/aug-cc-pVDZ ground-state calculations for nicotine ($C_{10}N_2H_{14}$, 402 MOs). Reported timings are wall times (t) per call, and we also report the number of calls. Calculations were performed using 20 cores with 2 TB memory available.

	e^T 1.0		e^T 2.0	
Operation	t	n_{calls}	t	n_{calls}
$\boldsymbol{\Omega}$ construction	48 min	10	41 min	5
$\boldsymbol{A}^T$ transformation	87 min	11	76 min	6
Determine $\boldsymbol{t}$ and $\bar{\boldsymbol{t}}$ amplitudes	24.7 h	⋯	12.4 h	⋯

TABLE VI. CC3/aug-cc-pVDZ excited-state calculations for nicotine ($C_{10}N_2H_{14}$, 402 MOs). Calculations were performed using 20 cores with 2 TB memory available.

	n_{calls}			
Operation	DIIS	Non-linear Davidson	Olsen	$t_{\boldsymbol{A}/\boldsymbol{A}^T}$
$\boldsymbol{A}$	8	20	8	80 min
$\boldsymbol{A}^T$	8	11	7	76 min
t_R (h)	11.3	27.9	12.8	
t_L (h)	11.0	15.6	10.8	

TABLE VII. Lowest ten singlet excitation energies of PSB3 calculated at the frozen-core CC3/aug-cc-pVDZ level of theory. Three different solvers have been used: DIIS, nonlinear Davidson, and multimodel Olsen. We also report the total time for the calculation of the excitation energies. The convergence threshold for the excited states is 10^{-3}. All energies are given in eV.

State	DIIS	Non-linear Davidson	Multimodel Olsen
1	4.1068	4.1059	4.1046
2	5.7480	5.7469	5.7436
3	6.3519	6.3509	6.3510
4	6.6510	6.6505	6.6504
5	7.0396	7.0383	7.0378
6	7.3710	7.3690	7.3693
7	7.3914	7.3924	7.3924
8	7.6928	7.6904	7.6903
9	7.7620	7.7024	7.7025
10	8.3043	7.7647	7.7645
Total time (h)	5.9	3.7	2.4

IV. COUPLED CLUSTER IMPLEMENTATION PERFORMANCE

The e^T program was originally a coupled cluster code, and the ability to perform efficient coupled cluster calculations remains among the most important features of the program. In this section, we demonstrate the capabilities of e^T 2.0 for standard coupled cluster calculations. We compare our current implementations to e^T 1.0 and other notable electronic structure software. The notation and relevant equations are defined in the Appendix. We use the default thresholds of e^T 2.0, unless stated otherwise: the Hartree–Fock equations are solved with a residual threshold of 10^{-7} a.u., Cholesky decomposition of the two-electron integrals is performed with a threshold of 10^{-4} a.u., and the coupled cluster ground- and excited-state equations are solved to residual thresholds of 10^{-5} and 10^{-3} a.u., respectively. For calculations with e^T 2.0, the default integral library (Libcint) is used. All timed calculations are performed on two Intel Xeon Platinum 8380 CPUs (2.30 GHz) with 2 TB shared memory, unless otherwise stated. All calculations are assigned 20 threads (or ten threads per CPU).

A. Comparing e^T 2.0 to e^T 1.0

Since the release of e^T 1.0, significant optimizations have been carried out in the coupled cluster implementations for the CC2, CCSD, and CC3 models. The improvements for CC3 are mainly due to the multimodel solvers, as detailed in Sec. III F. Here, we restrict our attention to CC2 and CCSD.

1. Calculations with the CC2 model

There are two implementations of the CC2 model in e^T, which differ in their memory requirements. The standard CC2 implementation has the same memory requirements as the CCSD implementation (tensors of dimension $n_o^2 n_v^2$ are kept in memory), while the *low-memory* CC2 implementation has an N^2 memory requirement, where N denotes the number of orbitals in the system. While both models have been optimized since e^T 1.0, the most significant optimizations have been implemented for low-memory CC2, where a looping strategy similar to that of the CC3 implementation[62,127] has been introduced.

In Table VIII, we report timings from a calculation of a single excitation energy of the erythromycin molecule ($C_{37}H_{67}O_{13}N$, 1719 MOs under the frozen core approximation; see Fig. 12(a). For erythromycin, the time to construct the $\boldsymbol{\Omega}$-vector [Eq. (A3)] and the linear transformation by the $\boldsymbol{A}$-matrix [to solve Eq. (A4)] has been reduced by factors of ~6 and ~4, respectively. The result is a significant reduction in the total computational times for the ground and excited states. Because different solvers are used (by default) in the two versions, the calculated excitation energies differ. In e^T 1.0, a DIIS solver was used for low-memory CC2. This solver does not ensure convergence to the roots with the lowest energy and is also prone to convergence of duplicate roots. In e^T 2.0, a nonlinear Davidson solver is used, ensuring no duplication of roots and convergence to the roots with the lowest energy (in molecules without symmetry).

2. Calculations with the CCSD model

We test the performance of the CCSD implementation with a calculation of the first four excited states for an azobenzene dye [$C_{24}H_{20}O_2N_4$, 822 MOs within the frozen core approximation, see Fig. 12(b)], and their transition strengths from the ground state; this provides the first features of the dye's ultraviolet spectrum. Here, we are primarily interested in the performance metrics and the comparison with e^T 1.0. Timings are given in Table IX.

The test consists of a ground-state and an excited-state calculation, where we need to determine the left and right amplitudes of both the ground state and the excited states [Eqs. (A12), (A3), (A9), (A4), and (A13)], and we present timings for each of these

TABLE VIII. Comparison of e^T 1.0 and e^T 2.0 CC2 ground- and excited-state calculations of erythromycin ($C_{37}H_{67}O_{13}N$, 1719 MOs under the frozen core approximation). We report the correlation energy (E_{corr}), the lowest excitation energy ω, and wall times to calculate the ground and excited states (t_{gs} and t_{es}), and the average times to construct the $\boldsymbol{\Omega}$ vector (t_Ω) and the linear transformation by the Jacobian matrix (t_A).

e^T	E_{corr} (E_h)	t_{gs} (h)	t_Ω (min)	ω (eV)	t_{es} (h)	t_A (h)
v1.0	−8.3934	7.1	36	5.1858	53.1	4.1
v2.0	−8.3934	1.8	6	4.0551	32.5	1.3

TABLE IX. Comparison of e^T 1.0 and e^T 2.0 CCSD/aug-cc-pVDZ ground- and excited-state calculations on the azobenzene dye ($C_{24}H_{20}O_2N_4$, 822 MOs within the frozen core approximation). Reported timings are wall times. Calculations were performed using 20 cores and 2 TB memory.

	e^T 1.0		e^T 2.0	
Total time	642.3 h		164.8 h	
	Ground state	Excited state	Ground state	Excited state
Left	29.3 h	336.3 h	11.8 h	24.4 h
Right	10.8 h	265.7 h	8.9 h	119.3 h

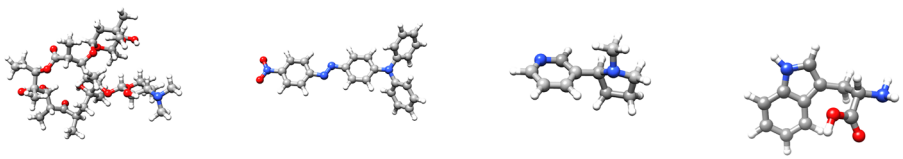

(a) (b) (c) (d)

FIG. 12. Molecules for performance testing of e^T plotted using UCSF Chimera:[98] (a) erythromycin, (b) azobenzene dye, (c) nicotine, and (d) tryptophan.

four steps. For the ground state, we observe only a modest performance improvement for the $\boldsymbol{t}$-amplitudes, whereas the $\bar{\boldsymbol{t}}$-amplitudes are obtained almost three times faster than in e^T 1.0. This speedup is primarily due to optimizations of the $\boldsymbol{A}^T$-transformation, which is more than twice as fast in e^T 2.0 compared to e^T 1.0.

For the excited states, we see speedups for both the right and the left amplitudes. The time per $\boldsymbol{A}$-transformation is almost halved compared to e^T 1.0. This is the primary cause of the speedup of the right excited states. For the left states, the speedup is due to both the optimizations of the $\boldsymbol{A}^T$-transformation and an improved starting guess; in e^T 2.0, the initial guess for the left amplitudes is generated from the converged right amplitudes. Overall, the optimizations for ground and excited states cut the total cost of the calculation by a factor of ~4 compared with e^T 1.0.

B. Comparisons to other electronic structure programs

We compare the CCSD implementation of e^T 2.0 to the electronic structure programs CFOUR,[2] Q-Chem (6.3),[13] and Psi4 (1.9.1),[15] all known for extensive coupled cluster functionality. For the latter two, Cholesky factorization of the electron repulsion integrals is used (with decomposition threshold τ). Psi4 is open source, whereas both CFOUR and Q-Chem are proprietary codes, with Q-Chem being commercial and CFOUR[2] being available for academic use upon request. Calculation input files can be found in Ref. 128.

In Table X, we present wall times for calculations of the first four excited states of nicotine using the aug-cc-pVDZ basis [$C_{10}H_{14}N_2$, 402 MOs; see Fig. 12(c)]. The wall times to solve the ground- and excited-state equations [Eqs. (A3) and (A4)] are given. The calculations are performed with either 200 GB or 2 TB of memory available; with 2 TB, all electron repulsion integrals can be stored in memory. Both e^T 2.0 and Q-Chem obtain four excited states of nicotine in 3–4 h, depending on the Cholesky decomposition threshold. While e^T solves the ground states more efficiently, Q-Chem is more efficient for the excited-state equations of this molecule.

In Table X, we also compare to the two coupled cluster programs included in the public release of CFOUR (ECC and NCC). The NCC program solves the excited-state equations in less than 4 h and is approximately twice as fast as the ECC program. However, the total wall time in all CFOUR calculations is high due to the integral transformations following the mean-field calculation; this bottleneck is eliminated in e^T and Q-Chem with the Cholesky decomposition of the integrals.

As the size of the molecular system increases, there is a crossover point at which e^T 2.0 becomes more efficient than the Q-Chem software. In Table XI, we compare Q-Chem to e^T 1.0 and e^T 2.0 for the first four excitations of tryptophan [$C_{11}H_{12}N_2O_2$, aug-cc-pVDZ, 438 MOs under the frozen core approximation, see Fig. 12(d)]. In these calculations, we calculate the energies and the transition strengths, that is, we solve Eqs. (A3), (A4), (A9), (A12), and (A13). From these calculations, we see that e^T 2.0 provides a significant improvement on the first release and that the first four excitation energies and transition strengths of tryptophan are obtained almost three times faster than with Q-Chem.

Finally, we compare the CC3 implementation of e^T 2.0 to the CC3 implementation of the NCC program in CFOUR. Previously, the CC3 implementation has been compared to the implementations in the Dalton program,[4] in the ECC program of CFOUR,[2] and in Psi4.[15,62] It was shown that e^T significantly outperformed the other implementations. From Table XII, where we present the calculation of a single excited state of nicotine, it is evident that both e^T and the NCC program provide efficient implementations of the CC3 model. With a Cholesky decomposition threshold of $\tau = 10^{-8}$, e^T 2.0 performs better under low-memory conditions, and CFOUR performs better under high-memory conditions, although the differences in performance are relatively minor. Note that the minimal memory

TABLE XI. CCSD/aug-cc-pVDZ ground- and excited-state calculation of tryptophan ($C_{11}H_{12}N_2O_2$, 438 MOs under the frozen core approximation). Cholesky-decomposed electron repulsion integrals are used, and the decomposition threshold is $\tau = 10^{-4}$.

	t_{gs} (h)	t_{es} (h)	t_{total} (h)	$n^{gs,R}_{calls}$	$n^{gs,L}_{calls}$	n^{R}_{calls}	n^{L}_{calls}
e^T 1.0	1.0	12.3	13.3	12	13	79	81
e^T 2.0	0.6	2.8	3.5	12	11	79	29
Q-Chem	1.8	7.9	10.0	13	8	83	24

TABLE X. CCSD/aug-cc-pVDZ calculations of the ground state and four excited states of nicotine ($C_{10}H_{14}N_2$, 402 MOs) using e^T, CFOUR, Q-Chem (6.3), and Psi4 (1.9.1). For e^T, Q-Chem, and Psi4, τ is the threshold for the Cholesky decomposition of the electron repulsion integrals. Calculations were performed using 20 cores, and the available memory is either 2 TB or 200 GB. Wall times for the ground state (t_{gs}), excited state (t_{es}), and the total calculation (t_{total}) is given in hours.

	2 TB							200 GB						
	Psi4	CFOUR		e^T 2.0		Q-Chem		Psi4	CFOUR		e^T 2.0		Q-Chem	
	$\tau = 10^{-4}$	ECC	NCC	$\tau = 10^{-4}$	$\tau = 10^{-8}$	$\tau = 10^{-4}$	$\tau = 10^{-8}$	$\tau = 10^{-4}$	ECC	NCC	$\tau = 10^{-4}$	$\tau = 10^{-8}$	$\tau = 10^{-4}$	$\tau = 10^{-8}$
t_{gs}	0.5[a]	0.7	0.3	0.3	0.5	0.6	0.8	0.5[a]	0.7	0.7	0.2	0.3	0.6	0.8
t_{es}	10.7	7.0	3.8	3.0	3.3	2.3	2.8	10.8	6.9	3.1	3.3	4.5	2.5	3.1
t_{tot}	11.2	12.3	8.6	3.3	3.9	3.1	3.8	11.8	12.1	8.3	3.5	4.8	3.1	3.9

[a]Ground-state equations are solved to (10^{-3}).

TABLE XII. CC3/aug-cc-pVDZ calculations of the ground state and a single excited state of nicotine ($C_{10}H_{14}N_2$, 402 MOs) using e^T and CFOUR. For e^T, we report timings with different Cholesky decomposition thresholds τ. The available memory is either 2 TB, 400 GB, or 200 GB.

Available memory	200 GB		400 GB			2 TB		
Program	e^T 2.0		CFOUR	e^T 2.0		CFOUR	e^T 2.0	
	$\tau = 10^{-4}$	$\tau = 10^{-8}$		$\tau = 10^{-4}$	$\tau = 10^{-8}$		$\tau = 10^{-4}$	$\tau = 10^{-8}$
Wall time (h)	208	210	226	209	214	198	210	210

requirement for CFOUR is 245 GB, whereas e^T 2.0 is able to run with less memory due to its batching algorithm[62] and never uses more than 427 GB in these calculations on nicotine.

V. FUTURE DEVELOPMENTS

The e^T program is a product of, and a framework for, significant and ongoing research activities within quantum chemistry. New functionality that reflects these activities will be introduced in the program. Below, we list some of the major ongoing developments that are underway.

Several recent developments in the code have targeted ground- and excited-state molecular dynamics, with recent developments of efficient analytical nuclear gradients and coupling elements at the CCSD[37,129] and similarity-constrained CCSD (SCCSD)[40,130–132] levels, which recently enabled nonadiabatic excited-state dynamics simulations with coupled cluster theory.[26,133] Very recent work has also made progress on the description of conical intersections at the CC2 level (SCC2),[134] determination of ground- and excited-state minimum-energy intersection geometries at the coupled cluster level,[135] as well as a correct description of ground-state intersections using the generalized coupled cluster (GCC)[136] and convex Hartree–Fock (CVX-HF)[137] methods. These developments are planned to be included in the next release, enabling the adoption of the developed methods for dynamics simulations.

Within multicomponent chemistry, additional functionality for conditions with strong light–matter coupling—such as triplet polaritonic states at the CCSD level of theory,[138] response theory for SC-QED-HF,[34,139] real-time time-dependent QED-CCSD,[81] as well as QED-HF harmonic frequencies (molecular gradients and Hessians)[39] and magnetic properties[140]—is underway. Recently, the QED implementations have been extended to treat chiral cavities[141,142] that enable the study of enantiomeric selectivity in ground and excited states. A model for collective strong coupling using QED-CCSD will be included in the next release.[143] Finally, additional wavefunction models, such as complete active space self-consistent field (CASSCF), QED–CASSCF,[144] and SC-QED-MP2,[32] and, in the context of electronically open molecules, the particle-breaking Hartree–Fock model[145,146] and its time-dependent version,[147] have been developed within the e^T community.

To study electronic excitations, time-dependent DFT (TDDFT) will soon be released,[148] in addition to new multilevel methods based on DFT.[44,45,149] This will allow for the study of large, realistic condensed-phase systems. To calculate local response properties, such as polarizabilities and electronic excitations, energy-based orbital localizations in specific fragment regions at the HF and DFT levels of theory[150–154] will allow for novel energy decomposition analysis.[151,154] Regarding the calculation of spectroscopic properties at the coupled cluster levels of theory, several upcoming features are in store. Resonant inelastic X-ray scattering (RIXS) spectroscopy[66] and X-ray emission spectroscopy (XES), implemented using a damped response solver (available in e^T 2.0), will soon be available. Transition moments will be available with the MLCC2 and MLCCSD models, as well as triplet excitation energies.

Another strand of developments in the code moves away from manual implementations of equations. Indeed, several upcoming developments in the program have been aided by the equation and e^T code generation tool SpinAdaptedSecondQuantization (SASQ).[155]

A significant emerging challenge for established electronic structure software, and also for the e^T program, is adapting to a further shift in HPC facilities toward heterogeneous computer architectures. Support for GPU acceleration and/or parallelization over multiple CPU/GPU nodes could be a necessary step to ensure that the e^T program remains competitive.

VI. CONCLUDING REMARKS

e^T 2.0 is an electronic structure program with an emphasis on efficiency and modularity, featuring efficient coupled cluster implementations and unique multicomponent and multilevel features. The program is open source and available to everyone free of cost, both for use and modification under the GPLv3.0 license conditions. The development cycle of the program is also open, with public code review and continuous improvements added to the development version hosted on GitLab. Rigorous testing and a continuous integration/continuous delivery (CI/CD) setup ensure that modifications are correct and that new additions follow style guidelines. Since the release of e^T 1.0, the program has undergone significant improvements. The coupled cluster implementations have been made more efficient with new solvers, improved starting guesses, and refinements in both memory handling and how terms are evaluated.

Since its first major release, the program has also evolved in new directions. Additional established mean-field and correlated models have been added to the program—such as ROHF, DFT, FCI,

and CASCI—and e^T has also been extended to treat new chemical and physical phenomena, such as strong light–matter coupling considered with the CBO approximation and at the mean-field and correlated levels of theory. With this major release, the e^T program is no longer only a coupled cluster code, even though it continues to prominently feature the functionality that gives the program its name.

ACKNOWLEDGMENTS

This work was supported by the European Research Council (ERC) under the European Union's Horizon 2020 Research and Innovation Program (Grant Agreement No. 101020016), the Marie Skłodowska-Curie European Training Network "COSINE - COmputational Spectroscopy In Natural Sciences and Engineering" (Grant Agreement No. 765739), and the Research Council of Norway through FRINATEK (Project Nos. 263110 and 275506). The work was also supported by advanced user support provided by Sigma2—the National Infrastructure for High-Performance Computing and Data Storage in Norway. J.P. and S.C. acknowledge financial support from the Technical University of Denmark within the Alliance Ph.D. Program. S.C. acknowledges financial support from the Independent Research Fund Denmark–Natural Sciences, Research Project 2 Grant No. 7014-00258B, and from the Novo Nordisk Foundation, Grant No. NNFSA220080996. T.G. acknowledges financial support from the European Union—Next Generation EU in the framework of the PRIN 2022 PNRR Project POSEIDON—Code No. P2022J9C3R. R.A., G.T., and E.R. acknowledge financial support from the European Research Council (ERC) under the European Union's Horizon 2020 Research and Innovation Program (Grant Agreement No. 101040197).

AUTHOR DECLARATIONS

Conflict of Interest

The authors have no conflicts to disclose.

Author Contributions

Sarai Dery Folkestad, Eirik F. Kjønstad, and Alexander C. Paul contributed equally to this work.

Sarai Dery Folkestad: Conceptualization (equal); Software (lead); Writing – original draft (lead); Writing – review & editing (lead). **Eirik F. Kjønstad**: Conceptualization (equal); Software (lead); Writing – original draft (equal); Writing – review & editing (equal). **Alexander C. Paul**: Conceptualization (equal); Software (lead); Writing – review & editing (supporting). **Rolf H. Myhre**: Conceptualization (supporting); Software (equal); Writing – review & editing (supporting). **Riccardo Alessandro**: Software (supporting); Writing – review & editing (supporting). **Sara Angelico**: Software (supporting); Writing – review & editing (supporting). **Alice Balbi**: Software (supporting); Writing – original draft (supporting); Writing – review & editing (supporting). **Alberto Barlini**: Software (supporting); Writing – review & editing (supporting). **Andrea Bianchi**: Software (supporting); Writing – review & editing (supporting). **Chiara Cappelli**: Software (supporting); Writing – review & editing (supporting). **Matteo Castagnola**: Software (supporting); Writing – review & editing (supporting). **Sonia Coriani**: Conceptualization (supporting); Software (supporting); Writing – review & editing (supporting). **Yassir El Moutaoukal**: Software (supporting); Writing – review & editing (supporting). **Tommaso Giovannini**: Software (supporting); Writing – review & editing (supporting). **Linda Goletto**: Software (supporting); Writing – review & editing (supporting). **Tor S. Haugland**: Software (supporting); Writing – review & editing (supporting). **Daniel Hollas**: Software (supporting); Writing – review & editing (supporting). **Ida-Marie Høyvik**: Software (supporting); Writing – review & editing (supporting). **Marcus T. Lexander**: Software (supporting); Writing – review & editing (supporting). **Doroteja Lipovec**: Software (supporting); Writing – review & editing (supporting). **Gioia Marrazzini**: Software (supporting); Writing – review & editing (supporting). **Torsha Moitra**: Software (supporting); Writing – review & editing (supporting). **Ylva Os**: Software (supporting); Writing – review & editing (supporting). **Regina Paul**: Software (supporting); Writing – review & editing (supporting). **Jacob Pedersen**: Software (supporting); Writing – review & editing (supporting). **Matteo Rinaldi**: Software (supporting); Writing – review & editing (supporting). **Rosario R. Riso**: Software (supporting); Writing – original draft (supporting); Writing – review & editing (supporting). **Sander Roet**: Software (supporting); Writing – review & editing (supporting). **Enrico Ronca**: Software (supporting); Writing – review & editing (supporting). **Federico Rossi**: Software (supporting); Writing – review & editing (supporting). **Bendik S. Sannes**: Software (supporting); Writing – review & editing (supporting). **Anna Kristina Schnack-Petersen**: Software (supporting); Writing – review & editing (supporting). **Andreas S. Skeidsvoll**: Software (supporting); Writing – review & editing (supporting). **Leo Stoll**: Software (supporting); Writing – review & editing (supporting). **Guillaume Thiam**: Software (supporting); Writing – review & editing (supporting). **Jan Haakon M. Trabski**: Software (supporting); Writing – review & editing (supporting). **Henrik Koch**: Conceptualization (lead); Software (supporting); Writing – original draft (equal); Writing – review & editing (equal).

DATA AVAILABILITY

The e^T program is available on GitLab (www.gitlab.com/eT-program/eT) and the user manual can be found on the program website, www.etprogram.org. Molecular geometries and output files for the reported calculations can be found in Ref. 128.

APPENDIX: SOLVING THE COUPLED CLUSTER EQUATIONS

In coupled cluster theory, the wavefunction is given by[156]

$$|\mathrm{CC}\rangle = \exp(T)|\mathrm{R}\rangle, \quad T = \sum_{\mu} t_\mu \tau_\mu, \tag{A1}$$

where $|\mathrm{HF}\rangle$ is the Hartree–Fock determinant, and T is the cluster operator that generates excitations of the reference determinant through excitation operators τ_μ. The ground-state coupled cluster equations are obtained by projecting the Schrödinger equation onto the Hartree–Fock state and excited configurations:

$$E_0 = \langle \mathrm{R}|\bar{H}|\mathrm{R}\rangle, \tag{A2}$$

$$\Omega_\mu = \langle \mu | \bar{H} | \mathrm{R} \rangle = 0. \tag{A3}$$

Here, we have introduced the similarity-transformed Hamiltonian $\bar{H} = \exp(-T) H \exp(T)$. The $\boldsymbol{\Omega}$-equations [Eq. (A3)] must be solved to determine the cluster amplitudes (t_μ).

Coupled cluster excitation energies can be calculated with linear response theory or the equation-of-motion (EOM) approach. In EOM coupled cluster theory, the states $|k\rangle$ are defined by the expansion,

$$|k\rangle = \sum_{\mu \geq 0} \exp(T) R_\mu^k |\mu\rangle, \tag{A4}$$

where $\boldsymbol{R}^k$ are the right eigenvectors of the similarity-transformed Hamiltonian:

$$\bar{\boldsymbol{H}} \boldsymbol{R}^k = E_k \boldsymbol{R}^k. \tag{A5}$$

The similarity-transformed Hamiltonian has the form

$$\bar{\boldsymbol{H}} = \begin{pmatrix} E_0 & \boldsymbol{\eta}^{\mathrm{T}} \\ \boldsymbol{\Omega} & \boldsymbol{A} + E_0 \boldsymbol{I} \end{pmatrix} = \begin{pmatrix} E_0 & \boldsymbol{\eta}^{\mathrm{T}} \\ \boldsymbol{0} & \boldsymbol{A} + E_0 \boldsymbol{I} \end{pmatrix}, \tag{A6}$$

where $\boldsymbol{A}$ is the Jacobian matrix with elements

$$A_{\mu\nu} = \langle \mu | [\bar{H}, \tau_\nu] | \mathrm{R} \rangle, \tag{A7}$$

and $\eta_\nu = \langle \mathrm{R} | [\bar{H}, \tau_\nu] | \mathrm{R} \rangle$. The eigenvalues of $\bar{\boldsymbol{H}}$ are the energies of the electronic states in EOM coupled cluster theory, and the excitation energies ω_k are the eigenvalues of $\boldsymbol{A}$.

The similarity-transformed Hamiltonian is non-Hermitian, and its left and right eigenvectors differ. We may express the left EOM coupled cluster states as

$$\langle k| = \sum_{\mu \geq 0} L_\mu^k \langle \mu | \exp(-T), \tag{A8}$$

where

$$\bar{\boldsymbol{H}}^{\mathrm{T}} \boldsymbol{L}^k = E_k \boldsymbol{L}^k, \tag{A9}$$

and we require that the left and right states form a biorthonormal set. With this biorthonormalization condition, the right vectors are given by

$$\boldsymbol{R}^0 = \begin{pmatrix} 1 \\ 0 \end{pmatrix}, \quad \boldsymbol{R}^k = \begin{pmatrix} \omega_k^{-1} \boldsymbol{\eta}^{\mathrm{T}} \boldsymbol{r}_k \\ \boldsymbol{r}_k \end{pmatrix} \quad \text{for } k > 0, \tag{A10}$$

where $\boldsymbol{r}_k$ are the right eigenvectors of $\boldsymbol{A}$, corresponding to the eigenvalue ω_k. The left vectors are given by

$$\boldsymbol{L}^0 = \begin{pmatrix} 1 \\ \bar{\boldsymbol{t}} \end{pmatrix}, \quad \boldsymbol{L}^k = \begin{pmatrix} 0 \\ \boldsymbol{l}_k \end{pmatrix} \quad \text{for } k > 0, \tag{A11}$$

where $\bar{\boldsymbol{t}}$ are the left ground-state amplitudes, determined by solving

$$\boldsymbol{A}^{\mathrm{T}} \bar{\boldsymbol{t}} = -\boldsymbol{\eta}, \tag{A12}$$

and $\boldsymbol{l}_k$ is a left eigenvector of $\boldsymbol{A}$, corresponding to the eigenvalue ω_k. The eigenvector equations for the Jacobian matrix and Eq. (A12) are solved using the linear transformation by $\boldsymbol{A}$ or its transpose. This transformation usually dominates the computational cost required to solve these equations.

Molecular response properties and oscillator strengths can also be obtained from linear response theory or within the EOM framework. For instance, the EOM oscillator strengths (for excitations from the ground state) are obtained from the expression

$$f_k = \frac{2}{3} \omega_k \langle 0 | \boldsymbol{\mu} | k \rangle \langle k | \boldsymbol{\mu} | 0 \rangle, \tag{A13}$$

which requires the calculation of left and right transition dipole moments.

REFERENCES

[1] M. J. Frisch, G. W. Trucks, H. B. Schlegel, G. E. Scuseria, M. A. Robb, J. R. Cheeseman, G. Scalmani, V. Barone, G. A. Petersson, H. Nakatsuji, X. Li, M. Caricato, A. V. Marenich, J. Bloino, B. G. Janesko, R. Gomperts, B. Mennucci, H. P. Hratchian, J. V. Ortiz, A. F. Izmaylov, J. L. Sonnenberg, D. Williams-Young, F. Ding, F. Lipparini, F. Egidi, J. Goings, B. Peng, A. Petrone, T. Henderson, D. Ranasinghe, V. G. Zakrzewski, J. Gao, N. Rega, G. Zheng, W. Liang, M. Hada, M. Ehara, K. Toyota, R. Fukuda, J. Hasegawa, M. Ishida, T. Nakajima, Y. Honda, O. Kitao, H. Nakai, T. Vreven, K. Throssell, J. A. Montgomery, Jr., J. E. Peralta, F. Ogliaro, M. J. Bearpark, J. J. Heyd, E. N. Brothers, K. N. Kudin, V. N. Staroverov, T. A. Keith, R. Kobayashi, J. Normand, K. Raghavachari, A. P. Rendell, J. C. Burant, S. S. Iyengar, J. Tomasi, M. Cossi, J. M. Millam, M. Klene, C. Adamo, R. Cammi, J. W. Ochterski, R. L. Martin, K. Morokuma, O. Farkas, J. B. Foresman, and D. J. Fox, Gaussian 16, Revision C.01, Gaussian, Inc., Wallingford, CT, 2016.

[2] D. A. Matthews, L. Cheng, M. E. Harding, F. Lipparini, S. Stopkowicz, T.-C. Jagau, P. G. Szalay, J. Gauss, and J. F. Stanton, "Coupled-cluster techniques for computational chemistry: The CFOUR program package," J. Chem. Phys. **152**, 214108 (2020).

[3] Q. Sun, X. Zhang, S. Banerjee, P. Bao, M. Barbry, N. S. Blunt, N. A. Bogdanov, G. H. Booth, J. Chen, Z.-H. Cui *et al.*, "Recent developments in the PySCF program package," J. Chem. Phys. **153**, 024109 (2020).

[4] K. Aidas, C. Angeli, K. L. Bak, V. Bakken, R. Bast, L. Boman, O. Christiansen, R. Cimiraglia, S. Coriani, P. Dahle *et al.*, "The Dalton quantum chemistry program system," Wiley Interdiscip. Rev.: Comput. Mol. Sci. **4**, 269–284 (2014).

[5] T. Saue, R. Bast, A. S. P. Gomes, H. J. A. Jensen, L. Visscher, I. A. Aucar, R. Di Remigio, K. G. Dyall, E. Eliav, E. Fasshauer *et al.*, "The DIRAC code for relativistic molecular calculations," J. Chem. Phys. **152**, 204104 (2020).

[6] N. Niemeyer, P. Eschenbach, M. Bensberg, J. Tölle, L. Hellmann, L. Lampe, A. Massolle, A. Rikus, D. Schnieders, J. P. Unsleber, and J. Neugebauer, "The subsystem quantum chemistry program Serenity," Wiley Interdiscip. Rev.: Comput. Mol. Sci. **13**, e1647 (2023).

[7] F. Zahariev, P. Xu, B. M. Westheimer, S. Webb, J. Galvez Vallejo, A. Tiwari, V. Sundriyal, M. Sosonkina, J. Shen, G. Schoendorff *et al.*, "The general atomic and molecular electronic structure system (GAMESS): Novel methods on novel architectures," J. Chem. Theory Comput. **19**, 7031–7055 (2023).

[8] S. G. Balasubramani, G. P. Chen, S. Coriani, M. Diedenhofen, M. S. Frank, Y. J. Franzke, F. Furche, R. Grotjahn, M. E. Harding, C. Hättig *et al.*, "TURBOMOLE: Modular program suite for *ab initio* quantum-chemical and condensed-matter simulations," J. Chem. Phys. **152**, 184107 (2020).

[9] Y. J. Franzke, C. Holzer, J. H. Andersen, T. Begušić, F. Bruder, S. Coriani, F. Della Sala, E. Fabiano, D. A. Fedotov, S. Fürst, S. Gillhuber, R. Grotjahn, M. Kaupp, M. Kehry, M. Krstić, F. Mack, S. Majumdar, B. D. Nguyen, S. M. Parker, F. Pauly, A. Pausch, E. Perlt, G. S. Phun, A. Rajabi, D. Rappoport, B. Samal, T. Schrader, M. Sharma, E. Tapavicza, R. S. Treß, V. Voora, A. Wodyński, J. M. Yu, B. Zerulla, F. Furche, C. Hättig, M. Sierka, D. P. Tew, and F. Weigend, "TURBOMOLE: Today and tomorrow," J. Chem. Theory Comput. **19**, 6859–6890 (2023).

[10] S. Seritan, C. Bannwarth, B. S. Fales, E. G. Hohenstein, S. I. L. Kokkila-Schumacher, N. Luehr, J. W. Snyder, C. Song, A. V. Titov, I. S. Ufimtsev, and T. J. Martínez, "TeraChem: Accelerating electronic structure and *ab initio* molecular dynamics with graphical processing units," J. Chem. Phys. **152**, 224110 (2020).

[11]N. Tancogne-Dejean, M. J. T. Oliveira, X. Andrade, H. Appel, C. H. Borca, G. Le Breton, F. Buchholz, A. Castro, S. Corni, A. A. Correa *et al.*, "Octopus, a computational framework for exploring light-driven phenomena and quantum dynamics in extended and finite systems," J. Chem. Phys. **152**, 124119 (2020).
[12]F. Neese, "Software update: The ORCA program system—version 6.0," Wiley Interdiscip. Rev.: Comput. Mol. Sci. **15**, e70019 (2025).
[13]E. Epifanovsky, A. T. B. Gilbert, X. Feng, J. Lee, Y. Mao, N. Mardirossian, P. Pokhilko, A. F. White, M. P. Coons, A. L. Dempwolff *et al.*, "Software for the frontiers of quantum chemistry: An overview of developments in the Q-Chem 5 package," J. Chem. Phys. **155**, 084801 (2021).
[14]K. Kowalski, R. Bair, N. P. Bauman, J. S. Boschen, E. J. Bylaska, J. Daily, W. A. de Jong, T. Dunning, Jr., N. Govind, R. J. Harrison *et al.*, "From NWChem to NWChemEx: Evolving with the computational chemistry landscape," Chem. Rev. **121**, 4962–4998 (2021).
[15]D. G. A. Smith, L. A. Burns, A. C. Simmonett, R. M. Parrish, M. C. Schieber, R. Galvelis, P. Kraus, H. Kruse, R. Di Remigio, A. Alenaizan *et al.*, "PSI4 1.4: Open-source software for high-throughput quantum chemistry," J. Chem. Phys. **152**, 184108 (2020).
[16]H.-J. Werner, P. J. Knowles, F. R. Manby, J. A. Black, K. Doll, A. Heßelmann, D. Kats, A. Köhn, T. Korona, D. A. Kreplin *et al.*, "The Molpro quantum chemistry package," J. Chem. Phys. **152**, 144107 (2020).
[17]M. Kállay, P. R. Nagy, D. Mester, Z. Rolik, G. Samu, J. Csontos, J. Csóka, P. B. Szabó, L. Gyevi-Nagy, B. Hégely *et al.*, "The MRCC program system: Accurate quantum chemistry from water to proteins," J. Chem. Phys. **152**, 074107 (2020).
[18]F. Aquilante, J. Autschbach, A. Baiardi, S. Battaglia, V. A. Borin, L. F. Chibotaru, I. Conti, L. De Vico, M. Delcey, I. Fdez Galván *et al.*, "Modern quantum chemistry with [Open]Molcas," J. Chem. Phys. **152**, 214117 (2020).
[19]G. Li Manni, I. F. Galván, A. Alavi, F. Aleotti, F. Aquilante, J. Autschbach, D. Avagliano, A. Baiardi, J. J. Bao, S. Battaglia, L. Birnoschi, A. Blanco-González, S. I. Bokarev, R. Broer, R. Cacciari, P. B. Calio, R. K. Carlson, R. Carvalho Couto, L. Cerdán, L. F. Chibotaru, N. F. Chilton, J. R. Church, I. Conti, S. Coriani, J. Cuéllar-Zuquin, R. E. Daoud, N. Dattani, P. Decleva, C. de Graaf, M. G. Delcey, L. De Vico, W. Dobrautz, S. S. Dong, R. Feng, N. Ferré, M. Filatov(Gulak), L. Gagliardi, M. Garavelli, L. González, Y. Guan, M. Guo, M. R. Hennefarth, M. R. Hermes, C. E. Hoyer, M. Huix-Rotllant, V. K. Jaiswal, A. Kaiser, D. S. Kaliakin, M. Khamesian, D. S. King, V. Kochetov, M. Krośnicki, A. A. Kumaar, E. D. Larsson, S. Lehtola, M.-B. Lepetit, H. Lischka, P. López Ríos, M. Lundberg, D. Ma, S. Mai, P. Marquetand, I. C. D. Merritt, F. Montorsi, M. Mörchen, A. Nenov, V. H. A. Nguyen, Y. Nishimoto, M. S. Oakley, M. Olivucci, M. Oppel, D. Padula, R. Pandharkar, Q. M. Phung, F. Plasser, G. Raggi, E. Rebolini, M. Reiher, I. Rivalta, D. Roca-Sanjuán, T. Romig, A. A. Safari, A. Sánchez-Mansilla, A. M. Sand, I. Schapiro, T. R. Scott, J. Segarra-Martí, F. Segatta, D.-C. Sergentu, P. Sharma, R. Shepard, Y. Shu, J. K. Staab, T. P. Straatsma, L. K. Sørensen, B. N. C. Tenorio, D. G. Truhlar, L. Ungur, M. Vacher, V. Veryazov, T. A. Voß, O. Weser, D. Wu, X. Yang, D. Yarkony, C. Zhou, J. P. Zobel, and R. Lindh, "The OpenMolcas *Web*: A community-driven approach to advancing computational chemistry," J. Chem. Theory Comput. **19**, 6933–6991 (2023).
[20]Z. Rinkevicius, X. Li, O. Vahtras, K. Ahmadzadeh, M. Brand, M. Ringholm, N. H. List, M. Scheurer, M. Scott, A. Dreuw, and P. Norman, "VeloxChem: A Python-driven density-functional theory program for spectroscopy simulations in high-performance computing environments," Wiley Interdiscip. Rev.: Comput. Mol. Sci. **10**, e1457 (2020).
[21]K. Boguslawski, F. Brzęk, R. Chakraborty, K. Cieślak, S. Jahani, A. Leszczyk, A. Nowak, E. Sujkowski, J. Świerczyński, S. Ahmadkhani *et al.*, "PyBEST: Improved functionality and enhanced performance," Comput. Phys. Commun. **297**, 109049 (2024).
[22]R. Di Felice, M. L. Mayes, R. M. Richard, D. B. Williams-Young, G. K.-L. Chan, W. A. de Jong, N. Govind, M. Head-Gordon, M. R. Hermes, K. Kowalski *et al.*, "A perspective on sustainable computational chemistry software development and integration," J. Chem. Theory Comput. **19**, 7056–7076 (2023).
[23]A. I. Krylov, J. M. Herbert, F. Furche, M. Head-Gordon, P. J. Knowles, R. Lindh, F. R. Manby, P. Pulay, C.-K. Skylaris, and H.-J. Werner, "What is the price of open-source software?," J. Phys. Chem. Lett. **6**, 2751–2754 (2015).
[24]S. Lehtola and A. J. Karttunen, "Free and open source software for computational chemistry education," Wiley Interdiscip. Rev.: Comput. Mol. Sci. **12**, e1610 (2022).
[25]*et docker*, https://gitlab.com/et-program/docker, 2026.
[26]E. F. Kjønstad, O. J. Fajen, A. C. Paul, S. Angelico, D. Mayer, M. Gühr, T. J. A. Wolf, T. J. Martínez, and H. Koch, "Photoinduced hydrogen dissociation in thymine predicted by coupled cluster theory," Nat. Commun. **15**, 10128 (2024).
[27]S. D. Folkestad, E. F. Kjønstad, R. H. Myhre, J. H. Andersen, A. Balbi, S. Coriani, T. Giovannini, L. Goletto, T. S. Haugland, A. Hutcheson, I.-M. Høyvik, T. Moitra, A. C. Paul, M. Scavino, A. S. Skeidsvoll, Å. H. Tveten, and H. Koch, "e^T 1.0: An open source electronic structure program with emphasis on coupled cluster and multilevel methods," J. Chem. Phys. **152**, 184103 (2020).
[28]T. S. Haugland, E. Ronca, E. F. Kjønstad, A. Rubio, and H. Koch, "Coupled cluster theory for molecular polaritons: Changing ground and excited states," Phys. Rev. X **10**, 041043 (2020).
[29]T. S. Haugland, C. Schäfer, E. Ronca, A. Rubio, and H. Koch, "Intermolecular interactions in optical cavities: An *ab initio* QED study," J. Chem. Phys. **154**, 094113 (2021).
[30]R. R. Riso, T. S. Haugland, E. Ronca, and H. Koch, "Molecular orbital theory in cavity QED environments," Nat. Commun. **13**, 1368 (2022).
[31]Y. El Moutaoukal, R. R. Riso, M. Castagnola, and H. Koch, "Toward polaritonic molecular orbitals for large molecular systems," J. Chem. Theory Comput. **20**, 8911–8920 (2024).
[32]Y. El Moutaoukal, R. R. Riso, M. Castagnola, E. Ronca, and H. Koch, "Strong coupling Møller-Plesset perturbation theory," J. Chem. Theory Comput. **21**, 3981–3992 (2025).
[33]S. Angelico, T. S. Haugland, E. Ronca, and H. Koch, "Coupled cluster cavity Born–Oppenheimer approximation for electronic strong coupling," J. Chem. Phys. **159**, 214112 (2023).
[34]M. Castagnola, R. R. Riso, A. Barlini, E. Ronca, and H. Koch, "Polaritonic response theory for exact and approximate wave functions," Wiley Interdiscip. Rev.: Comput. Mol. Sci. **14**, e1684 (2024).
[35]J. Fregoni, T. S. Haugland, S. Pipolo, T. Giovannini, H. Koch, and S. Corni, "Strong coupling between localized surface plasmons and molecules by coupled cluster theory," Nano Lett. **21**, 6664–6670 (2021).
[36]M. Romanelli, R. R. Riso, T. S. Haugland, E. Ronca, S. Corni, and H. Koch, "Effective single-mode methodology for strongly coupled multimode molecular-plasmon nanosystems," Nano Lett. **23**, 4938–4946 (2023).
[37]A. K. Schnack-Petersen, H. Koch, S. Coriani, and E. F. Kjønstad, "Efficient implementation of molecular CCSD gradients with Cholesky-decomposed electron repulsion integrals," J. Chem. Phys. **156**, 244111 (2022).
[38]M. T. Lexander, J. H. M. Trabski, A. Bianchi, E. F. Kjønstad, T. S. Haugland, and H. Koch, "Exploring molecular equilibrium geometries in static and quantized fields," J. Chem. Theory Comput. **21**, 10157–10165 (2025).
[39]A. Barlini, A. Bianchi, J. H. M. Trabski, J. Bloino, and H. Koch, "Cavity field-driven symmetry breaking and modulation of vibrational properties: Insights from the analytical QED-HF hessian," J. Chem. Theory Comput. **21**, 9323–9334 (2025).
[40]M. T. Lexander, S. Angelico, E. F. Kjønstad, and H. Koch, "Analytical evaluation of ground state gradients in quantum electrodynamics coupled cluster theory," J. Chem. Theory Comput. **20**, 8876–8885 (2024).
[41]A. S. Skeidsvoll, A. Balbi, and H. Koch, "Time-dependent coupled-cluster theory for ultrafast transient-absorption spectroscopy," Phys. Rev. A **102**, 023115 (2020).
[42]A. S. Skeidsvoll, T. Moitra, A. Balbi, A. C. Paul, S. Coriani, and H. Koch, "Simulating weak-field attosecond processes with a Lanczos reduced basis approach to time-dependent equation-of-motion coupled-cluster theory," Phys. Rev. A **105**, 023103 (2022).
[43]T. Tsuchimochi and G. E. Scuseria, "Communication: ROHF theory made simple," J. Chem. Phys. **133**, 141102 (2010).
[44]G. Marrazzini, T. Giovannini, M. Scavino, F. Egidi, C. Cappelli, and H. Koch, "Multilevel density functional theory," J. Chem. Theory Comput. **17**, 791–803 (2021).
[45]T. Giovannini, G. Marrazzini, M. Scavino, H. Koch, and C. Cappelli, "Integrated multiscale multilevel approach to open shell molecular systems," J. Chem. Theory Comput. **19**, 1446–1456 (2023).
[46]V. I. Lebedev and D. N. Laikov, "A quadrature formula for the sphere of the 131st algebraic order of accuracy," in *Doklady Mathematics* (Pleiades Publishing Ltd., 1999), Vol. 59, pp. 477–481.

[47]M. Krack and A. M. Köster, "An adaptive numerical integrator for molecular integrals," J. Chem. Phys. **108**, 3226–3234 (1998).
[48]Q. Sun, "Libcint: An efficient general integral library for Gaussian basis functions," J. Comput. Chem. **36**, 1664–1671 (2015).
[49]E. Valeyev, K. Surjuse, L. A. Burns, A. Abbott, E. Kawashima, P. Seewald, J. Misiewicz, D. Lewis, J. Calvin, J. Dullea, C. Peng, A. Asadchev, A. Panyala, K. Nishimra, M. Clement, S. Slattery, J. Fermann, S. Lehtola, M. F. Herbst, D. Mejia-Rodriguez, E. Mitchell, O. Čertík, R. Ellerbrock, J. D. Whitfield, A. Wingate, B. M. Wiedemann, F. Bosia, M. Banck, and S. Y. Willow (2025). "Evaleev/libint: 2.11.1," Zenodo. https://doi.org/10.5281/zenodo.18463981
[50]A. Bianchi (2025). "Phasedint," Zenodo. https://zenodo.org/records/17025111
[51]R. Di Remigio, A. H. Steindal, K. Mozgawa, V. Weijo, H. Cao, and L. Frediani, "PCMSolver: An open-source library for solvation modeling," Int. J. Quantum Chem. **119**, e25685 (2019).
[52]S. Lehtola, C. Steigemann, M. J. T. Oliveira, and M. A. L. Marques, "Recent developments in LIBXC—A comprehensive library of functionals for density functional theory," SoftwareX **7**, 1–5 (2018).
[53]M. A. L. Marques, M. J. T. Oliveira, and T. Burnus, "LIBXC: A library of exchange and correlation functionals for density functional theory," Comput. Phys. Commun. **183**, 2272–2281 (2012).
[54]R. Fletcher, *Practical Methods of Optimization* (John Wiley & Sons, 2013).
[55]P. Jørgensen, P. Swanstrøm, and D. L. Yeager, "Guaranteed convergence in ground state multiconfigurational self-consistent field calculations," J. Chem. Phys. **78**, 347–356 (1983).
[56]I.-M. Høyvik, B. Jansik, and P. Jørgensen, "Trust region minimization of orbital localization functions," J. Chem. Theory Comput. **8**, 3137–3146 (2012).
[57]S. D. Folkestad, R. Matveeva, I.-M. Høyvik, and H. Koch, "Implementation of occupied and virtual Edmiston–Ruedenberg orbitals using Cholesky decomposed integrals," J. Chem. Theory Comput. **18**, 4733–4744 (2022).
[58]E. R. Davidson, "The iterative calculation of a few of the lowest eigenvalues and corresponding eigenvectors of large real-symmetric matrices," J. Comput. Phys. **17**, 87–94 (1975).
[59]K. Hirao and H. Nakatsuji, "A generalization of the Davidson's method to large nonsymmetric eigenvalue problems," J. Comput. Phys. **45**, 246–254 (1982).
[60]O. Christiansen, H. Koch, and P. Jørgensen, "The second-order approximate coupled cluster singles and doubles model CC2," Chem. Phys. Lett. **243**, 409–418 (1995).
[61]H. Koch, O. Christiansen, A. M. Sanchez de Merás, T. Helgaker *et al.*, "The CC3 model: An iterative coupled cluster approach including connected triples," J. Chem. Phys. **106**, 1808–1818 (1997).
[62]A. C. Paul, R. H. Myhre, and H. Koch, "New and efficient implementation of CC3," J. Chem. Theory Comput. **17**, 117–126 (2020).
[63]G. E. Scuseria, T. J. Lee, and H. F. Schaefer, "Accelerating the convergence of the coupled-cluster approach: The use of the DIIS method," Chem. Phys. Lett. **130**, 236–239 (1986).
[64]T. P. Hamilton and P. Pulay, "Direct inversion in the iterative subspace (DIIS) optimization of open-shell, excited-state, and small multiconfiguration SCF wave functions," J. Chem. Phys. **84**, 5728–5734 (1986).
[65]E. F. Kjønstad, S. D. Folkestad, and H. Koch, "Accelerated multimodel newton-type algorithms for faster convergence of ground and excited state coupled cluster equations," J. Chem. Phys. **153**, 014104 (2020).
[66]A. K. Schnack-Petersen, T. Moitra, S. D. Folkestad, and S. Coriani, "New implementation of an equation-of-motion coupled-cluster damped-response framework with illustrative applications to resonant inelastic X-ray scattering," J. Phys. Chem. A **127**, 1775–1793 (2023).
[67]*Coveralls*, https://coveralls.io, 2026.
[68]R. Bast (2018). "Runtest," Zenodo.https://doi.org/10.5281/zenodo.1434751
[69]M. Rilee and T. Clune, "Towards test driven development for computational science with pFUnit," in *2014 Second International Workshop on Software Engineering for High Performance Computing in Computational Science and Engineering* (IEEE, 2014), pp. 20–27.
[70]J. Bloch, A. Cavalleri, V. Galitski, M. Hafezi, and A. Rubio, "Strongly correlated electron–photon systems," Nature **606**, 41–48 (2022).
[71]J. Fregoni, F. J. Garcia-Vidal, and J. Feist, "Theoretical challenges in polaritonic chemistry," ACS Photonics **9**, 1096–1107 (2022).
[72]M. Ruggenthaler, D. Sidler, and A. Rubio, "Understanding polaritonic chemistry from ab initio quantum electrodynamics," Chem. Rev. **123**, 11191–11229 (2023).
[73]J. Feist, J. Galego, and F. J. Garcia-Vidal, "Polaritonic chemistry with organic molecules," ACS Photonics **5**, 205–216 (2018).
[74]C. Schäfer, J. Fojt, E. Lindgren, and P. Erhart, "Machine learning for polaritonic chemistry: Accessing chemical kinetics," J. Am. Chem. Soc. **146**, 5402–5413 (2024).
[75]J. George and J. Singh, "Polaritonic chemistry: Band-selective control of chemical reactions by vibrational strong coupling," ACS Catal. **13**, 2631–2636 (2023).
[76]T. W. Ebbesen, A. Rubio, and G. D. Scholes, "Introduction: Polaritonic chemistry," Chem. Rev. **123**, 12037–12038 (2023).
[77]J. A. Campos-Gonzalez-Angulo, R. F. Ribeiro, and J. Yuen-Zhou, "Resonant catalysis of thermally activated chemical reactions with vibrational polaritons," Nat. Commun. **10**, 4685 (2019).
[78]D. Wellnitz, G. Pupillo, and J. Schachenmayer, "Disorder enhanced vibrational entanglement and dynamics in polaritonic chemistry," Commun. Phys. **5**, 120 (2022).
[79]K. Nagarajan, A. Thomas, and T. W. Ebbesen, "Chemistry under vibrational strong coupling," J. Am. Chem. Soc. **143**, 16877–16889 (2021).
[80]F. J. Garcia-Vidal, C. Ciuti, and T. W. Ebbesen, "Manipulating matter by strong coupling to vacuum fields," Science **373**, eabd0336 (2021).
[81]M. Castagnola, M. T. Lexander, E. Ronca, and H. Koch, "Strong coupling electron-photon dynamics: A real-time investigation of energy redistribution in molecular polaritons," Phys. Rev. Res. **6**, 033283 (2024).
[82]G. Sandik, J. Feist, F. J. García-Vidal, and T. Schwartz, "Cavity-enhanced energy transport in molecular systems," Nat. Mater. **24**, 344–355 (2024).
[83]R. Chikkaraddy, B. de Nijs, F. Benz, S. J. Barrow, O. A. Scherman, E. Rosta, A. Demetriadou, P. Fox, O. Hess, and J. J. Baumberg, "Single-molecule strong coupling at room temperature in plasmonic nanocavities," Nature **535**, 127–130 (2016).
[84]K. Santhosh, O. Bitton, L. Chuntonov, and G. Haran, "Vacuum rabi splitting in a plasmonic cavity at the single quantum emitter limit," Nat. Commun. **7**, ncomms11823 (2016).
[85]W. Wu, Y. Battie, C. Genet, T. W. Ebbesen, G. Decher, and M. Pauly, "Bottom-up tunable broadband semi-reflective chiral mirrors," Adv. Opt. Mater. **11**, 2202831 (2023).
[86]A. Thomas, L. Lethuillier-Karl, K. Nagarajan, R. M. A. Vergauwe, J. George, T. Chervy, A. Shalabney, E. Devaux, C. Genet, J. Moran, and T. W. Ebbesen, "Tilting a ground-state reactivity landscape by vibrational strong coupling," Science **363**, 615–619 (2019).
[87]J. A. Hutchison, T. Schwartz, C. Genet, E. Devaux, and T. W. Ebbesen, "Modifying chemical landscapes by coupling to vacuum fields," Angew. Chem., Int. Ed. **51**, 1592–1596 (2012).
[88]A. Thomas, J. George, A. Shalabney, M. Dryzhakov, S. J. Varma, J. Moran, T. Chervy, X. Zhong, E. Devaux, C. Genet *et al.*, "Ground-state chemical reactivity under vibrational coupling to the vacuum electromagnetic field," Angew. Chem. **128**, 11634–11638 (2016).
[89]W. Ahn, J. F. Triana, F. Recabal, F. Herrera, and B. S. Simpkins, "Modification of ground-state chemical reactivity via light–matter coherence in infrared cavities," Science **380**, 1165–1168 (2023).
[90]M. V. Imperatore, J. B. Asbury, and N. C. Giebink, "Reproducibility of cavity-enhanced chemical reaction rates in the vibrational strong coupling regime," J. Chem. Phys. **154**, 191103 (2021).
[91]M. Ruggenthaler, J. Flick, C. Pellegrini, H. Appel, I. V. Tokatly, and A. Rubio, "Quantum-electrodynamical density-functional theory: Bridging quantum optics and electronic-structure theory," Phys. Rev. A **90**, 012508 (2014).
[92]J. Flick, M. Ruggenthaler, H. Appel, and A. Rubio, "Kohn–Sham approach to quantum electrodynamical density-functional theory: Exact time-dependent effective potentials in real space," Proc. Natl. Acad. Sci. U. S. A. **112**, 15285–15290 (2015).
[93]I.-T. Lu, M. Ruggenthaler, N. Tancogne-Dejean, S. Latini, M. Penz, and A. Rubio, "Electron-photon exchange-correlation approximation for quantum-electrodynamical density-functional theory," Phys. Rev. A **109**, 052823 (2024).

[94]A. Balbi, A. S. Skeidsvoll, and H. Koch, "Coupled cluster simulation of impulsive stimulated x-ray raman scattering," J. Phys. Chem. A **127**, 8676–8684 (2023).
[95]A. S. Skeidsvoll and H. Koch, "Comparing real-time coupled-cluster methods through simulation of collective Rabi oscillations," Phys. Rev. A **108**, 033116 (2023).
[96]J. R. Dormand and P. J. Prince, "A family of embedded Runge-Kutta formulae," J. Comput. Appl. Math. **6**, 19–26 (1980).
[97]E. Hairer, G. Wanner, and S. P. Nørsett, "Runge-Kutta and extrapolation methods," in *Solving Ordinary Differential Equations I: Nonstiff Problems* (Springer, Berlin, Heidelberg, 1993), pp. 129–353.
[98]E. F. Pettersen, T. D. Goddard, C. C. Huang, G. S. Couch, D. M. Greenblatt, E. C. Meng, and T. E. Ferrin, "UCSF Chimera–A visualization system for exploratory research and analysis," J. Comput. Chem. **25**, 1605–1612 (2004).
[99]P. C. Hariharan and J. A. Pople, "The influence of polarization functions on molecular orbital hydrogenation energies," Theor. Chim. Acta **28**, 213–222 (1973).
[100]V. Bakken and T. Helgaker, "The efficient optimization of molecular geometries using redundant internal coordinates," J. Chem. Phys. **117**, 9160–9174 (2002).
[101]L.-P. Wang and C. Song, "Geometry optimization made simple with translation and rotation coordinates," J. Chem. Phys. **144**, 214108 (2016).
[102]S. Coriani and H. Koch, "Communication: X-ray absorption spectra and core-ionization potentials within a core-valence separated coupled cluster framework," J. Chem. Phys. **143**, 181103 (2015).
[103]S. Coriani and H. Koch, "Erratum: 'Communication: X-ray absorption spectra and core-ionization potentials within a core-valence separated coupled cluster framework' [J. Chem. Phys. 143, 181103 (2015)]," J. Chem. Phys. **145**, 149901 (2016).
[104]R. Arneberg, J. Müller, and R. Manne, "Configuration interaction calculations of satellite structure in photoelectron spectra of H_2O," Chem. Phys. **64**, 249–258 (1982).
[105]C. M. Oana and A. I. Krylov, "Dyson orbitals for ionization from the ground and electronically excited states within equation-of-motion coupled-cluster formalism: Theory, implementation, and examples," J. Chem. Phys. **127**, 234106 (2007).
[106]J. V. Ortiz, "Dyson-orbital concepts for description of electrons in molecules," J. Chem. Phys. **153**, 070902 (2020).
[107]A. I. Krylov, "From orbitals to observables and back," J. Chem. Phys. **153**, 080901 (2020).
[108]T. Moitra, A. C. Paul, P. Decleva, H. Koch, and S. Coriani, "Multi-electron excitation contributions towards primary and satellite states in the photoelectron spectrum," Phys. Chem. Chem. Phys. **24**, 8329–8343 (2022).
[109]B. F. E. Curchod and T. J. Martínez, "Ab initio nonadiabatic quantum molecular dynamics," Chem. Rev. **118**, 3305–3336 (2018).
[110]I.-M. Høyvik, R. H. Myhre, and H. Koch, "Correlated natural transition orbitals for core excitation energies in multilevel coupled cluster models," J. Chem. Phys. **146**, 144109 (2017).
[111]S. D. Folkestad and H. Koch, "Multilevel CC2 and CCSD methods with correlated natural transition orbitals," J. Chem. Theory Comput. **16**, 179–189 (2019).
[112]H. M. Senn and W. Thiel, "QM/MM methods for biomolecular systems," Angew. Chem., Int. Ed. **48**, 1198–1229 (2009).
[113]J. Tomasi, B. Mennucci, and R. Cammi, "Quantum mechanical continuum solvation models," Chem. Rev. **105**, 2999–3094 (2005).
[114]A. Warshel and M. Karplus, "Calculation of ground and excited state potential surfaces of conjugated molecules. I. Formulation and parametrization," J. Am. Chem. Soc. **94**, 5612–5625 (1972).
[115]A. Warshel and M. Levitt, "Theoretical studies of enzymic reactions: Dielectric, electrostatic and steric stabilization of the carbonium ion in the reaction of lysozyme," J. Mol. Biol. **103**, 227–249 (1976).
[116]T. A. Wesolowski and A. Warshel, "Frozen density functional approach for ab initio calculations of solvated molecules," J. Phys. Chem. **97**, 8050–8053 (1993).
[117]J. Tomasi, R. Cammi, B. Mennucci, C. Cappelli, and S. Corni, "Molecular properties in solution described with a continuum solvation model," Phys. Chem. Chem. Phys. **4**, 5697–5712 (2002).
[118]C. Cappelli, "Integrated QM/polarizable MM/continuum approaches to model chiroptical properties of strongly interacting solute-solvent systems," Int. J. Quantum Chem. **116**, 1532–1542 (2016).
[119]T. Giovannini, F. Egidi, and C. Cappelli, "Molecular spectroscopy of aqueous solutions: A theoretical perspective," Chem. Soc. Rev. **49**, 5664–5677 (2020).
[120]T. Giovannini, F. Egidi, and C. Cappelli, "Theory and algorithms for chiroptical properties and spectroscopies of aqueous systems," Phys. Chem. Chem. Phys. **22**, 22864–22879 (2020).
[121]S. D. Folkestad, A. C. Paul, R. Paul, S. Coriani, M. Odelius, M. Iannuzzi, and H. Koch, "Understanding x-ray absorption in liquid water using triple excitations in multilevel coupled cluster theory," Nat. Commun. **15**, 3551 (2024).
[122]S. D. Folkestad, A. C. Paul, R. Paul née Matveeva, P. Reinholdt, S. Coriani, M. Odelius, and H. Koch, "Quantum mechanical versus polarizable embedding schemes: A study of the x-ray absorption spectra of aqueous ammonia and ammonium," J. Chem. Theory Comput. **20**, 4161–4169 (2024).
[123]T. Giovannini, S. Gómez, and C. Cappelli, "Modeling Raman spectra in complex environments: From solutions to surface-enhanced Raman scattering," J. Phys. Chem. Lett. **16**, 3106–3121 (2025).
[124]S. D. Folkestad, E. F. Kjønstad, and H. Koch, "An efficient algorithm for Cholesky decomposition of electron repulsion integrals," J. Chem. Phys. **150**, 194112 (2019).
[125]S. D. Folkestad, E. F. Kjønstad, L. Goletto, and H. Koch, "Multilevel CC2 and CCSD in reduced orbital spaces: Electronic excitations in large molecular systems," J. Chem. Theory Comput. **17**, 714–726 (2021).
[126]J. Olsen, P. Jørgensen, and J. Simons, "Passing the one-billion limit in full configuration-interaction (FCI) calculations," Chem. Phys. Lett. **169**, 463–472 (1990).
[127]R. H. Myhre and H. Koch, "The multilevel CC3 coupled cluster model," J. Chem. Phys. **145**, 044111 (2016).
[128]eT-Program Developers (2025). "Geometries and outputs for 'eT 2.0 An efficient open-source molecular electronic structure program'," Zenodo. https://doi.org/10.5281/zenodo.17314762
[129]E. F. Kjønstad and H. Koch, "Communication: Non-adiabatic derivative coupling elements for the coupled cluster singles and doubles model," J. Chem. Phys. **158**, 161106 (2023).
[130]E. F. Kjønstad and H. Koch, "Resolving the notorious case of conical intersections for coupled cluster dynamics," J. Phys. Chem. Lett. **8**, 4801–4807 (2017).
[131]E. F. Kjønstad and H. Koch, "An orbital invariant similarity constrained coupled cluster model," J. Chem. Theory Comput. **15**, 5386–5397 (2019).
[132]E. F. Kjønstad, S. Angelico, and H. Koch, "Coupled cluster theory for nonadiabatic dynamics: Nuclear gradients and nonadiabatic couplings in similarity constrained coupled cluster theory," J. Chem. Theory Comput. **20**, 7080–7092 (2024).
[133]D. Hait, D. Lahana, O. J. Fajen, A. S. P. Paz, P. A. Unzueta, B. Rana, L. Lu, Y. Wang, E. F. Kjønstad, H. Koch, and T. J. Martínez, "Prediction of photodynamics of 200 nm excited cyclobutanone with linear response electronic structure and ab initio multiple spawning," J. Chem. Phys. **160**, 244101 (2024).
[134]L. Stoll, S. Angelico, E. F. Kjønstad, and H. Koch, "Similarity constrained CC2: Toward efficient coupled cluster nonadiabatic dynamics among excited states," J. Chem. Theory Comput. **21**, 10466–10473 (2025).
[135]S. Angelico, E. F. Kjønstad, and H. Koch, "Determining minimum energy conical intersections by enveloping the seam: Exploring ground and excited state intersections in coupled cluster theory," J. Phys. Chem. Lett. **16**, 561–567 (2025).
[136]F. Rossi, E. F. Kjønstad, S. Angelico, and H. Koch, "Generalized coupled cluster theory for ground and excited state intersections," J. Phys. Chem. Lett. **16**, 568–578 (2025).
[137]F. Rossi and H. Koch, "Convex Hartree–Fock theory for modeling ground state conical intersections," Commun. Chem. **9**, 32 (2026).
[138]W. H. Smedsrud, "Coupled-cluster equation of motion method (QED-CCSD-1) for triplet excitations in optical cavities," M.S. thesis, NTNU, 2024.
[139]M. Castagnola, R. R. Riso, Y. El Moutaoukal, E. Ronca, and H. Koch, "Strong coupling quantum electrodynamics Hartree–Fock response theory," J. Phys. Chem. A **129**, 4447–4457 (2025).

[140]A. Barlini, A. Bianchi, E. Ronca, and H. Koch, "Theory of magnetic properties in quantum electrodynamics environments: Application to molecular aromaticity," J. Chem. Theory Comput. **20**, 7841–7854 (2024).
[141]R. R. Riso, L. Grazioli, E. Ronca, T. Giovannini, and H. Koch, "Strong coupling in chiral cavities: Nonperturbative framework for enantiomer discrimination," Phys. Rev. X **13**, 031002 (2023).
[142]R. R. Riso, M. Castagnola, E. Ronca, and H. Koch, "Chiral polaritonics: Cavity-mediated enantioselective excitation condensation," Rep. Prog. Phys. **88**, 027901 (2025).
[143]M. Castagnola, M. T. Lexander, and H. Koch, "Realistic *ab initio* predictions of excimer behavior under collective light-matter strong coupling," Phys. Rev. X **15**, 021040 (2025).
[144]R. Alessandro, M. Castagnola, H. Koch, and E. Ronca, "A complete active space self-consistent field approach for molecules in QED environments," J. Chem. Theory Comput. **21**, 6862–6873 (2025).
[145]R. Matveeva, S. D. Folkestad, and I.-M. Høyvik, "Particle-breaking Hartree–Fock theory for open molecular systems," J. Phys. Chem. A **127**, 1329–1341 (2023).
[146]R. Paul née Matveeva, S. D. Folkestad, B. S. Sannes, and I.-M. Høyvik, "Particle-breaking unrestricted Hartree–Fock theory for open molecular systems," J. Phys. Chem. A **128**, 1533–1542 (2024).
[147]J. Pedersen, B. S. Sannes, R. Paul née Matveeva, S. Coriani, and I.-M. Høyvik, "Time-dependent particle-breaking Hartree–Fock model for electronically open molecules," J. Phys. Chem. A **129**, 4288–4300 (2025).
[148]M. A. L. Marques and E. K. U. Gross, "Time-dependent density functional theory," Annu. Rev. Phys. Chem. **55**, 427–455 (2004).
[149]T. Giovannini, M. Scavino, and H. Koch, "Time-dependent multi-level density functional theory," J. Chem. Theory Comput. **20**, 3601–3612 (2024).
[150]T. Giovannini and H. Koch, "Energy-based molecular orbital localization in a specific spatial region," J. Chem. Theory Comput. **17**, 139–150 (2020).
[151]T. Giovannini and H. Koch, "Fragment localized molecular orbitals," J. Chem. Theory Comput. **18**, 4806–4813 (2022).
[152]L. Goletto, S. Gómez, J. H. Andersen, H. Koch, and T. Giovannini, "Linear response properties of solvated systems: A computational study," Phys. Chem. Chem. Phys. **24**, 27866–27878 (2022).
[153]L. Goletto, T. Giovannini, S. D. Folkestad, and H. Koch, "Combining multilevel Hartree–Fock and multilevel coupled cluster approaches with molecular mechanics: A study of electronic excitations in solutions," Phys. Chem. Chem. Phys. **23**, 4413–4425 (2021).
[154]T. Giovannini, "Kohn–Sham fragment energy decomposition analysis," J. Chem. Phys. **161**, 104110 (2024).
[155]M. T. Lexander, T. S. Haugland, F. Rossi, and H. Koch, "SpinAdaptedSecondQuantization.jl 1.0—A simple and pedagogical approach to symbolic quantum chemistry," J. Phys. Chem. A **129**, 11053–11062 (2025).
[156]T. Helgaker, P. Jørgensen, and J. Olsen, *Molecular Electronic-Structure Theory* (John Wiley & Sons, 2014).